CHEMICAL REVIEWS

REVIEW

pubs.acs.org/CR

Rational Synthesis of Noncentrosymmetric Metal−Organic Frameworks for Second-Order Nonlinear Optics

Cheng Wang,[†] Teng Zhang,[†] and Wenbin Lin*

Department of Chemistry, CB#3290, University of North Carolina, Chapel Hill, North Carolina 27599, United States

CONTENTS

1. INTRODUCTION TO NONLINEAR OPTICS

The term nonlinear optics (NLO) was coined to describe the nonlinear relationship between dielectric polarization **P** and electric field **E** in optical media. NLO is a cornerstone of the emerging field of photonics, in which photons instead of electrons are used for signal transmission and processing.[1,2] The vision of photonic signal transmission, processing, and storage has attracted a great deal of attention from both the engineering and the scientific communities because of its great impact in many of the existing and future information technologies.

The first step toward realization of these revolutionary technologies is to develop tools to manipulate photons. For example, it is desirable to develop materials with the ability to alter the frequency of light, to amplify light signal, and to modulate light intensity or phase factors. NLO phenomena can be the key to achieving these important functions. One of the most common NLO behaviors is second-harmonic generation (SHG), in which a NLO material mediates the "adding-up" of two photons to form a new one with twice the frequency. The SHG phenomenon was first demonstrated by Franken et al. in 1961.[3] In their pioneering work, a laser beam with a wavelength of 694.2 nm was irradiated through a quartz crystal and an output ultraviolet radiation with a wavelength of 347.1 nm (double frequency) was detected. After this discovery, numerous nonlinear optical phenomena have been studied and a number of NLO-active materials have been developed.[1]

Second-harmonic generation can be quantitatively described by the second-order nonlinear optical susceptibility $\chi^{(2)}$, a third-rank tensor with 27 components. The tensor elements are related to each other to meet the requirements of both inherent and structural symmetries, which greatly reduces the number of independent components of the susceptibility tensor. Only crystals in noncentrosymmetric crystal classes can have nonvanishing $\chi^{(2)}$.[4,5] Moreover, for material crystallizing in the noncentrosymmetric 422, 622, and 432 crystal classes, the second-order NLO response might also vanish due to structural symmetry as well as Kleinman's symmetry.[6]

Many inorganic compounds crystallize in noncentrosymmetric space groups and have been found to be SHG active. Some important examples are potassium dihydrogen phosphate (KDP = KH_2PO_4), lithium niobate ($LiNbO_3$), and barium sodium niobate ($Ba_2NaNb_5O_{15}$).[7] New inorganic compounds have been explored for NLO applications including but not limited to metal borates[8−12] and metal oxides.[13,14] Recent structural studies on the inorganic systems have led to a better understanding of crystal growth/packing, paving the way for potentially manipulating their crystallization tendency to form noncentrosymmetric structures.[15,16]

Since the 1970s molecular NLO materials, including organic, organometallic, and inorganic complexes, have been of increasing interest to synthetic chemists.[17−19] The existing library of organic compounds was first screened, and the urea crystal has become a SHG standard because of its high SHG efficiency and usual availability.[7] In a microscopic view, the second-order NLO susceptibility $\chi^{(2)}$ is related to the first hyperpolarizability β of a molecule. According to the classical two-level model, β is enhanced by a large transition moment and a large dipole moment difference between the ground and the charge transfer excited state.[20] A donor−acceptor type of molecule often possesses both a large transition moment and a large excited state dipole moment. As a result, most of the organic SHG chromophors belong to this category.[21] However, most of the molecules with large β values also possess a large dipole moment, which induces formation of centrosymmetric assemblies of molecules due to dipole−dipole interactions.[22] One of the methods to avoid the centrosymmetric alignment of molecular dipoles is to trap them inside the channels of asymmetric porous host structures.[23−28] Other methods include formation of poled polymers in which the required asymmetry is imposed by the external electric field[7,29−35] and the Langmuir−Blodgett (LB)

Special Issue: 2012 Metal-Organic Frameworks

Received: July 7, 2011
Published: November 09, 2011

film method in which the intrinsic asymmetry of the surface is utilized.[36−39] Self-assembled superlattices, representing one of the most delicate structural controls of the surface, can also lead to NLO active materials.[40−46]

SHG of NLO active materials has found the most common use in the laser industry. For example, SHG can be used to generate the green 532 nm laser from a 1064 nm Nd:YAG infrared (IR) laser source. In high-quality diode lasers, the bulk KDP crystal is placed in front of the laser source and an infrared filter is coated on the output side of the crystal to prevent leakage of intense 1064 or 808 nm (the light source to pump the Nd:YAG laser) near-IR light. Green laser pointers commonly found in lecture halls adopt the same design, except that the expensive infrared filter is not always used, which raises safety concerns. By taking advantage of the frequency doubling property of a NLO material, high-intensity deep-UV light can be generated from a regular UV laser source. Laser pulses with wavelengths down to 166 nm have been generated in this way.[1] The difference frequency generation property of some NLO materials has been used in the generation of terahertz waves, in which the frequencies of a pair of IR photons are subtracted from each other to obtain radiation in the terahertz range.[1] On the other hand, the phase-matching effect of SHG crystals can be utilized to obtain compressed ultrashort laser pulses.[1]

NLO materials have already been used in optoelectronic technologies. An optical frequency multiplier is a nonlinear optical device which uses NLO materials to combine two photons to a new one with a higher frequency. An optical parametric amplifier (OPA) is a laser light source that emits light of variable wavelengths, in which the photon of an incident laser pulse (pump) is divided into two photons called a signal and an idler through a NLO crystal. In a similar device called an optical parametric oscillator (OPO) a NLO crystal is assembled together with an optical resonator with enhanced NLO effects. OPOs are widely used in laser spectroscopy.[47] An electro-optic rectifier is a device which involves generation of a quasi-DC polarization in a NLO crystal when intense optical beams are passing through, resembling the voltage gate in an electronic rectifier.[48] All these devices serve as building blocks for construction of optical transistors and photonic logic gates in future optical computers and other photonic integrated circuit systems.[2] These NLO devices are also readily incorporated into advanced optical communication systems.

Last but not the least, SHG effect is used for high-resolution optical microscopy in biological and medical applications. Collagen, which is found in the flesh and most connective tissues, exhibits SHG activity. This allows imaging of cornea[49] and lamina cribrosa sclera[50] by SHG microscopy with very high axial and lateral resolutions.

Several methods have been developed to determine absolute or relative values of the second-order NLO susceptibility $\chi^{(2)}$. These methods, including the phase-matched method, parametric fluorescence,[51] Raman scattering,[52] the Maker fringe method,[53] and the wedge method, were carefully reviewed by Kurtz in 1975.[54] In most cases when accurate results are not required, the less quantitative Kurtz-Perry method[55] is used. The Kurtz-Perry method allows one to determine the NLO properties of a polycrystalline sample and is of great value as a screening technique. A typical setup of the Kurtz-Perry method is shown in Figure 1.[56] The sample, a polycrystalline powder (~50 mg), is packed in a cell and irradiated with a long-wavelength (low-energy) laser. The SHG intensity is measured by a photomultiplier tube (PMT).[7,56] The results are usually compared with a standard material such as α-quartz, KDP, or urea. KDP has an efficiency of 16 × α-quartz,[57] while urea has an efficiency of 400 × α-quartz. The technologically important $LiNbO_3$ is 600 × α-quartz.

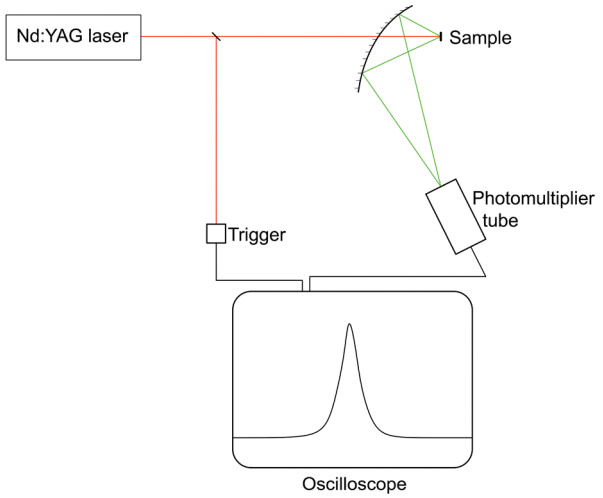

Figure 1. Schematic diagram of a Kurtz powder test setup.

The SHG intensity is particle-size dependent. Figure 2 shows the dependence of $I(2\omega)$ on particle size in both phase-matchable and nonphase-matchable cases.[56] In type 1 phase-matched cases (e.g., $LiNbO_3$), the SHG intensity increases with the particle size and eventually reaches a plateau. If phase matching does not occur (e.g., quartz), the intensity will first increase and then decrease as the particle size increases, and a maximum value can be reached. Therefore, SHG measurements as a function of particle size are necessary for more accurate and reliable results.

2. DESIGN AND SYNTHESIS OF SHG-ACTIVE MOFS

Metal−organic frameworks (MOFs), previously known as coordination polymers or coordination networks (here we use MOF as a synonym to coordination polymer, which includes 1-D, 2-D, and 3-D infinite structures), have emerged as an interesting class of inorganic−organic hybrid materials which can be fine tuned at the molecular level.[58,59] The modular nature of MOF synthesis has allowed systematic structural design and incorporation of various functionalities, leading to a variety of MOFs with potential applications in gas storage,[60] chemical sensing,[61−63] catalysis,[64,65] biomedical imaging,[66−68] and drug delivery.[69,70] MOFs are also readily characterized by X-ray crystallography, which facilitates establishment of structure−property relationships. SHG generation was one of the first active functions that were rationally designed based on MOFs. This review aims to summarize the progress toward rational synthesis of noncentrosymmetric MOFs with SHG properties in recent years.

Unlike organic molecular crystals or traditional inorganic materials, noncentrosymmetric MOFs can be rationally designed and synthesized, taking advantage of the well-defined geometry of metal centers and highly directional metal−ligand coordination bonds. With a combination of crystal engineering and synthetic chemistry, noncentrosymmetric networks can be designed and synthesized in a systematic way to give rise to a new category of potential NLO materials.[22]

In this section, we will discuss the design principle and examples of SHG-active MOFs in the literature. After a brief

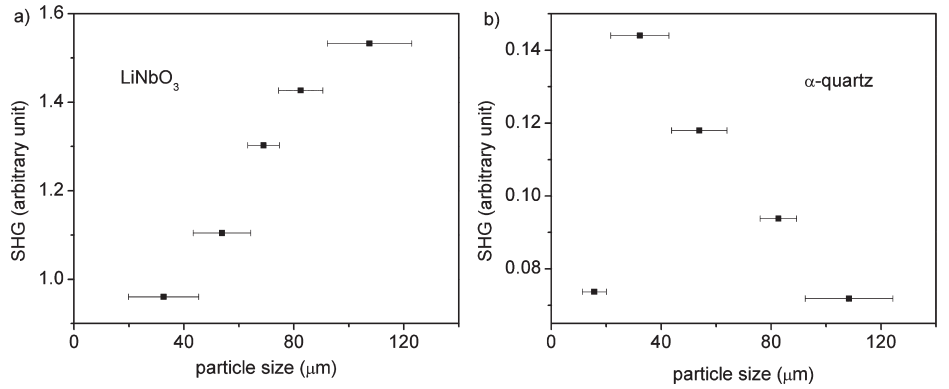

Figure 2. Dependence of SHG activity and particle size in (a) phase-matchable ($LiNbO_3$) and (b) nonphase-matchable (α-quartz) cases. Reprinted with permission from ref 56. Copyright 2006 The Royal Society of Chemistry.

Table 1. SHG-Active MOFs with 3-D Diamondoid Structures

MOF	chemical formula	space group	folds	SHG($I^{2\omega}$)	ref
1	$Zn(inic)_2$	$P2_12_12_1$	3	1.5 × α-quartz	74
4	$Zn(4\text{-}pya)_2$	Cc	5	126 × α-quartz	77
6	$Cd(pyb)_2 \cdot H_2O$	Cc	5	18 × α-quartz	74,77
8	$Cd(4\text{-}pya)_2 \cdot H_2O$	Ia	7	310 × α-quartz	77
9	$Zn((E)\text{-}4\text{-}pyv\text{-}4\text{-}bza)_2$	$C2$	8	400 × α-quartz	76
10	$Cd((E)\text{-}4\text{-}pyv\text{-}4\text{-}bza)_2$	$C2$	8	345 × α-quartz	76
11	$Zn(imac)_2 \cdot H_2O$	Cc	5	3 × KDP	78
12	$(Me_2NH_2)[CdLi(odba)_2]$	$I\bar{4}2d$	5	5 × KDP	79
13	$Zn(ima)_2$	Cc	3	0.5 × urea	80
14	Zn(3-pya)(OH)	$P2_12_12_1$	1	active	87
15	$(H_2NMe_2)(NH_4)$ $[Cd(3,3'\text{-}AZDB)_2]$	$C222_1$	6	1.2 × urea	88
16	$Zn(phtz)_2$	$I\bar{4}2d$	1	1 × urea	83
17	$Zn(aptz)_2$	$I\bar{4}2d$	1	4 × urea	83
18	$Zn(3\text{-}ptz)_2$	$I\bar{4}2d$	1	0.4× urea	84
19	Zn(tzb)	$Pca2_1$	1	0.5 × KDP	82
20	$Cd_2(tcsm)(DMA)_2(H_2O)_2$	$I\bar{4}$	7	1.1 × KDP	85
21	$Zn_2(tcom)(CH_3CH_2OH) \cdot 3H_2O$	Cc	3	2.5 × KDP	86

discussion of the choice of metal nodes in MOF synthesis, SHG-active MOFs in the literature are categorized into six groups based on their design geometry or principle: 3-D diamondoid frameworks, other 3-D frameworks, octupolar MOFs, 2-D frameworks, 1-D chains, and MOFs built from chiral ligands.

2.1. Choice of Metal Nodes

In order to minimize optical losses in SHG processes, optical materials need to be transparent in the working frequency range. To avoid unwanted d−d transitions in the visible region, d^{10} metal ions are commonly used as connecting points in nonlinear optically active MOFs. The most widely used connecting metals are Zn^{2+} and Cd^{2+}. Both of these metals can have tetrahedral or pseudotetrahedral coordination extensions, which intrinsically lacks a center of symmetry. They can also form complicated clusters with various coordination ligands to form 1-D to 3-D MOFs.

Ag^+ and Cu^+ are another set of d^{10} metals for construction of transparent MOFs for NLO applications. However, the Ag(I) and Cu(I) centers can be easily oxidized or reduced under MOF synthesis conditions. In addition, the lower coordination numbers of the Ag(I) and Cu(I) centers tend to afford MOFs of lower dimensionality, which diminishes the chance of obtaining noncentrosymmetric materials.

Mn^{2+} ions with the d^5 electronic configuration have also been used to construct SHG-active MOFs. Due to the spin-forbidden d−d transition of d^5 metal ions, Mn MOFs are fairly optically transparent and often just slightly pink. Mn(II) MOFs can still be explored for NLO applications as a result of their small optical loss in the visible spectrum.

Main group metals have also been used for construction of SHG-active MOFs. Mg^{2+} has been used in a MOF built from benzene-1,3,5-tricarboxylate ligands, which showed moderate SHG activity.[71] MOFs containing Pb^{2+} and In^{3+} ions have also been reported to be SHG active.[72,73] However, main group MOFs tend to exhibit lower stability, which represents a significant drawback for their NLO applications.

2.2. 3-D Diamondoid Structures

A diamondoid network has been identified as a topological motif with a strong tendency to afford noncentrosymmetric structures (Table 1).[22,74] The diamond crystal (A4) itself

dx.doi.org/10.1021/cr200252n |*Chem. Rev.* 2012, 112, 1084–1104

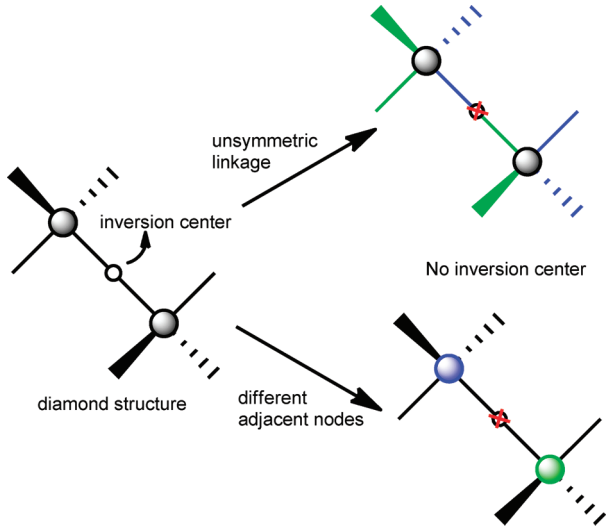

Figure 3. Two ways to remove inversion centers in diamondoid structures: (top) using unsymmetrical linkage and (bottom) using different adjacent nodes.

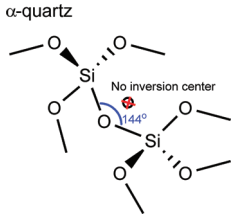

Figure 4. Loss of the center of symmetry in α-quartz as a result of the V-shaped Si−O−Si linkage.

crystallizes in a centrosymmetric space group ($Fd\bar{3}m$), as a result of the inversion center residing at the middle of the C−C linkage between adjacent nodes. There are thus two ways to break the center of symmetry in diamond nets: (1) using unsymmetrical bridging ligands to connect the tetrahedral nodes and (2) using different adjacent connecting nodes (Figure 3).

The simplest example of breaking the centrosymmetry of a diamond net using an unsymmetrical bridging ligand is illustrated in α-quartz. Adopting the diamondoid topology, α-quartz has a Si−O−Si bond angle of 144°, leading to a V-shaped linkage between two adjacent Si atoms and resulting in a noncentrosymmetric structure (Figure 4). α-Quartz crystallizes in a pair of chiral enantiomorphous space groups $P3_121$ and $P3_221$ and exhibits activity in SHG.

Lin and co-workers pioneered the use of tetrahedral metal centers (Zn^{2+}, Cd^{2+}) and unsymmetrical linear bridging ligands (such as *p*-pyridinecarboxylate and its derivatives) for construction of noncentrosymmetric MOFs of the diamondoid topology (Figure 6). The unsymmetrical bridging ligands not only eliminate the center of symmetry in the coordination network but also introduce electronic asymmetry, which is the key to high hyperpolarizability. The crystals were synthesized by hydro(solvo)thermal techniques, with in-situ generation of the pyridinecarboxylate linking ligands from cyano or ester precursors under the reaction conditions (Figure 5).[22]

Lin et al. first synthesized bis(isonicotinato) zinc, **1**, via a solvothermal reaction between $Zn(ClO_4)_2\cdot 6H_2O$ and 4-cyanopyridine at 130 °C.[74] **1** exhibits a diamondoid structure with 3-fold interpenetration (Figure 7) and crystallizes in the chiral space group $P2_12_12_1$. The tetraheral Zn^{2+} centers in **1** coordinate to two pyridine groups and two monodentate carboxylate groups of four different isonicotinate ligands, leading to a noncentrosymmetric framework. The SHG signal of **1** was determined to be 1.5 times more intense than that of α-quartz based on Kurtz powder tests.

Similar reactions between $Cd(ClO_4)_2\cdot 6H_2O$ and 4-cyanopyridine yielded two more diamondoid MOFs **2** and **3**.[75] However, both **2** and **3** adopt 2-fold interpenetrations, presumably because Cd^{2+} ions prefer a higher coordination number than Zn^{2+} ions and form bulkier connecting nodes that reduce the room left for interpenetration. Each Cd^{2+} coordinates to two pyridine groups, two bidentate carboxylate groups, and one solvent molecule, also leading to a noncentrosymmetric diamondoid network. Crystals of MOFs **2** and **3**, however, crystallize in centrosymmetric space groups, owing to the fact that the two interpenetrating nets are related through the inversion symmetry to each other (Figure 8). Although an individual diamondoid network is noncentrosymmetric, even-number-fold of intepenetration can still lead to a centrosymmetric crystal. An odd-number-fold interpenetration, on the other hand, must retain the noncentrosymmetric nature of individual nets.

Lin et al. further demonstrated the ability to crystal engineer noncentrosymmetric MOFs of the diamondoid topology by tuning the length of *p*-pyridinecarboxylate linkers. Hydro(solvo)thermal reactions between $Zn(ClO_4)_2\cdot 6H_2O$ or $Cd(ClO_4)_2\cdot 6H_2O$ and the corresponding precursors of unsymmetrical linking ligands $\mathbf{L_{2-5}}$ (Figure 5) afforded a series of MOFs of the diamondoid topology with systematically elongated linear spacers (Figures 9 and 10). Rational synthesis of this archetypical series of isoreticular MOFs convincingly demonstrated the feasibility of designing functional materials via a combination of molecular and crystal engineering.[74,76,77]

As the void space within a single diamondoid network gets larger with a longer bridging ligand, a larger number of the networks can be fitted into the space to lead to a higher degree of interpenetration. $Zn(4\text{-pya})_2$, **4**, and $[Cd(4\text{-pya})_2](H_2O)$, **6** [where 4-pya = (*E*)-3-(pyridin-4-yl)acrylate], both adopt a 5-fold interpenetrated diamondoid network structure and crystallize in noncentrosymmetric space group *Cc* (Figure 9).[77] The even longer 4-(4-pyridyl)benzoate and 4-[2-(4-pyridyl)ethenyl]benzoate ligands led to diamondoid structures with 7- and 8-fold interpenetration, respectively (Figure 10, **8**−**10**).[76,77] The even-number-fold interpenetration does not prevent **10** from crystallizing in the chiral space group *C*2.

A linear relationship between the degree of interpenetration of diamondoid networks and the length of bridging *p*-pyridinecarboxyalte ligands was established for the isoreticular diamondoid MOF series (Figure 11).[22] The work by Lin et al. thus convincingly demonstrated the ability to crystal engineer noncentrosymmetric MOFs by simply choosing bridging ligands of appropriate lengths. Importantly, noncentrosymmetric diamondoid MOFs **1**−**10** exhibited impressive SHG activities. Lin et al. also observed that in the isoreticular MOF series the longer the bridging ligand the higher the SHG efficiency. This trend is expected since the longer bridging ligands exhibit better conjugation between the donor and the acceptor, which is known to enhance the molecular hyperpolarizability of NLO chromophores. It is also notable that the SHG properties of **9** and **10** built from the long $\mathbf{L_5}$ ligand are comparable to that of the technologically important lithium niobate material. On the basis of the same design principle, Yao et al.,[78] Du et al.,[79] and

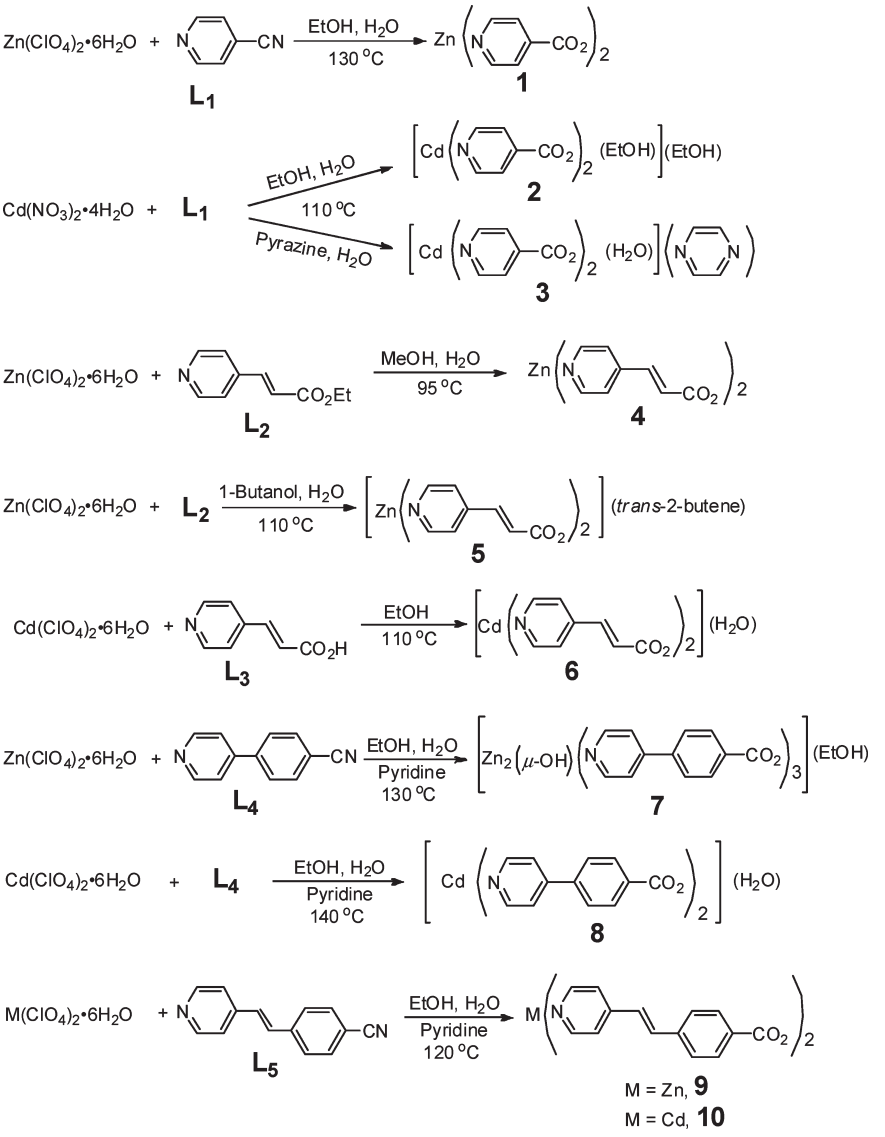

Figure 5. Synthesis of 3-D diamondoid MOFs using the *p*-pyridinecarboxylate ligands. Reprinted with permission from ref 22. Copyright 2002 American Chemcial Society.

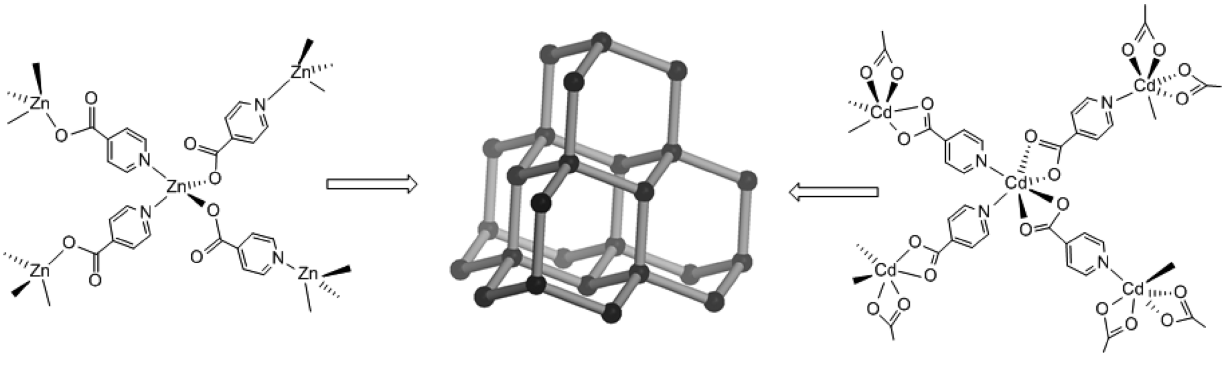

Figure 6. 3-D MOFs of diamondoid topology built from Zn^{2+} or Cd^{2+} tetrahedral connecting points and *p*-pyridinecarboxylate linkers.

Wang et al.[80] constructed diamondoid MOFs (**11**−**15**) from ditopic imidazolcarboxylate ligand and Zn^{2+} ions, which were found to crystallize in noncentrosymmetric space groups and to be SHG active.

Xiong et al. extended the in-situ ligand synthesis strategy first developed in the Lin group to prepare Zn−tetrazole MOFs by reacting nitriles, sodium azide, and Zn^{2+} salts under

dx.doi.org/10.1021/cr200252n |*Chem. Rev.* 2012, 112, 1084–1104

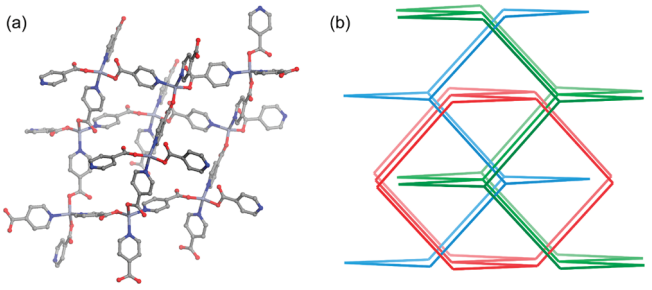

Figure 7. (a) View of the diamondoid network of **1**. (b) Diagram showing the 3-fold interpenetration in **1**.

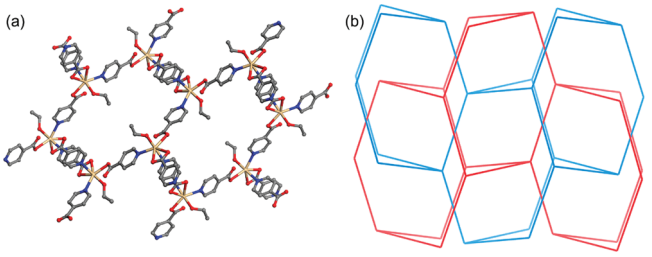

Figure 8. (a) View of the diamondoid network of **2**. Coordinating ethanol molecules were omitted for clarity. (b) Diagram showing the 2-fold interpenetration in **2**, leading to the center of symmetry in the structure.

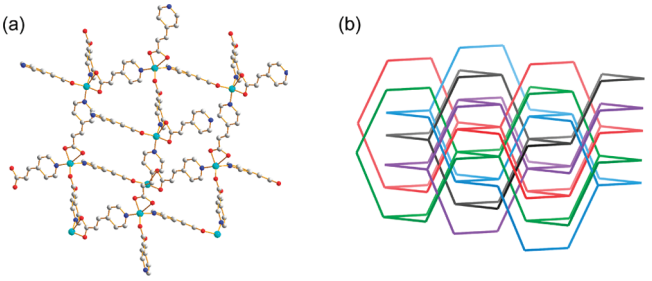

Figure 9. (a) View of the diamondoid network of **4**. (b) Diagram showing the 5-fold interpenetration in **4** and **6**.

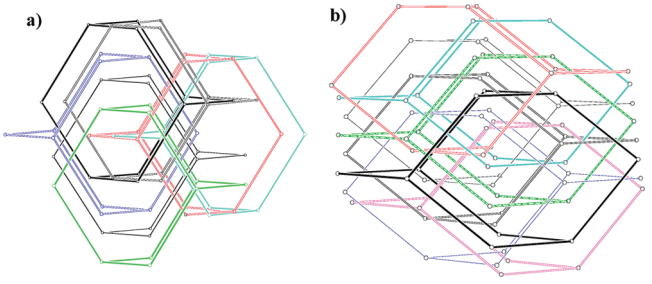

Figure 10. (a) Diagram showing the 7-fold interpenetration in **8**. (b) Diagram showing the 8-fold interpenetration in **9** and **10**. Reprinted with permission from ref 77. Copyright 2001 American Chemical Society.

hydro(solvo)thermal conditions.[81] When the tetrazoles are in ditopic coordination modes they can serve as a linear spacer to link the tetrahedral d^{10} metal nodes to form diamondoid structures. A combination of shorter Zn···Zn separations and the

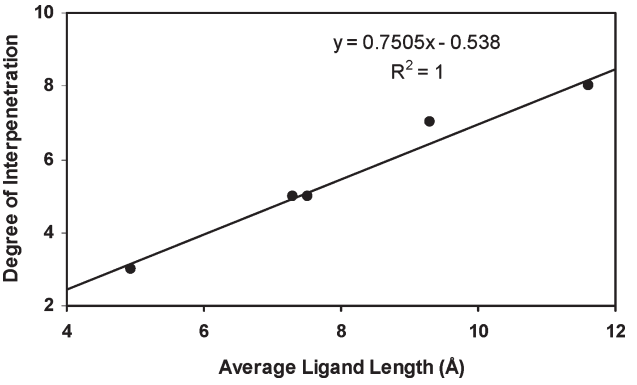

Figure 11. Dependence of the degree of interpenetration of diamondoid networks on the length of bridging *p*-pyridinecarboxylate ligands. Reprinted with permission from ref 22. Copyright 2002 American Chemical Society. Reprinted with permission from ref 22. Copyright 2002 American Chemical Society.

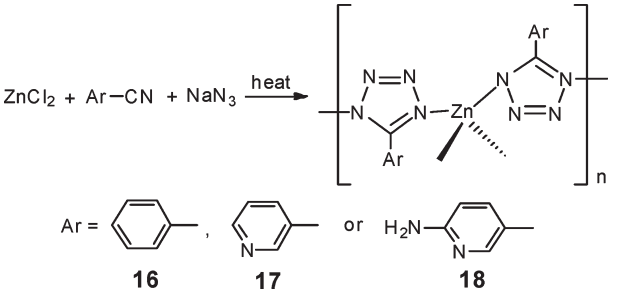

Figure 12. Synthesis of Zn diamondoid networks based on the in-situ-generated tetrazole bridging ligands.

large R groups on the tetrazole bridging ligands precludes interpenetration in these Zn−tetrazole diamondoid MOFs. Three noninterpenetrated diamondoid MOFs **16**−**19** were synthesized using this strategy (Figures 12 and 13), and all of them showed substantial SHG responses.[82−84]

Inverse design of noncentrosymmetric diamondoid MOFs is also possible by switching the roles of the metal centers and bridging ligands. In a diamondoid MOF (**20**) reported by Liang et al.[85] a tetracarboxylate ligand, tetrakis(4-(carboxylatostyrenyl))methane, serves as the 4-connected node as a result of the tetrahedral geometry of the sp^3 carbon at the center whereas the Cd^{2+} ion acts as an unsymmetrical ditopic connector (Figure 14). The Cd^{2+} ion coordinates to two bidentate carboxylates and two solvent molecules (DMF and water), leading to an octahedral coordinating environment. Although such noncentrosymmetric diamondoid MOFs can be designed, they are not expected to exhibit large SHG activity owing to the lack of electronic asymmetry in the building blocks.

As mentioned above, noncentrosymmetric diamondoid MOFs can also be constructed by making the adjacent tetrahedral nodes different (strictly speaking, such a structure belongs to the cubic-ZnS net). This strategy was employed by Guo et al.[86] using tetracarboxylate and tetratopic clusters of zinc to construct cross-linked noncentrosymmetric diamondoid MOF **21** (Figure 14). This diamondoid structure is built from two kinds of tetrahedral nodes: one-half of them are the sp^3 carbons of the methane-derived ligands, and the other half of them are the 4-connected metal clusters. Any nodes in the structures are

dx.doi.org/10.1021/cr200252n |*Chem. Rev.* 2012, 112, 1084–1104

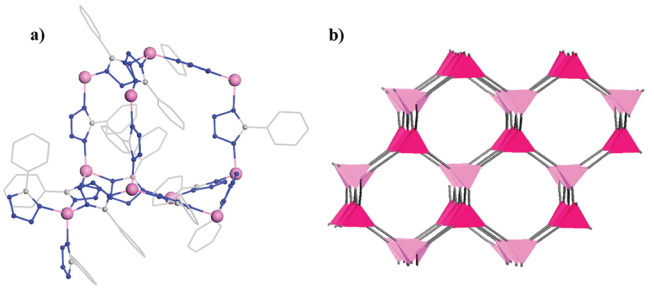

Figure 13. (a) View of the diamondoid network of **16**. (b) Diagram showing the diamondoid network of **16** with tetrahedra representing the Zn coordination environments. Reprinted with permission from ref 83. Copyright 2005 American Chemical Society.

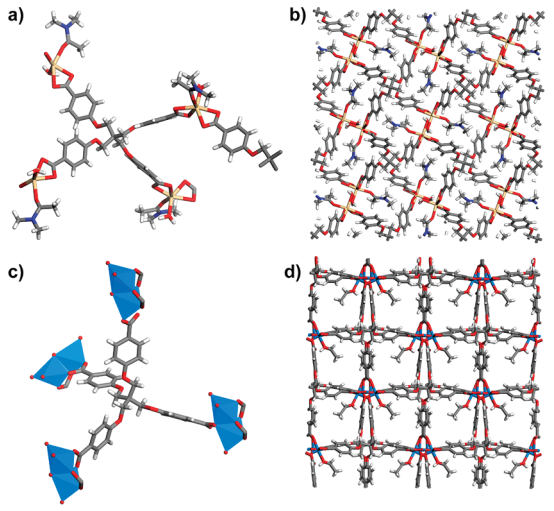

Figure 14. (a) Tetrahedral building blocks of **20** with tetracarboxylate extended from sp^3 carbon and 2-connected Cd centers. (b) Seven-fold interpenetrating diamondoid structure of **20**. (c) Tetrahedral building blocks of **21**. (d) Three-fold interpenetrating diamondoid structure of **21**.

necessarily adjacent to the other kind by design, thus eliminating the inversion center of the parent diamond structure.

2.3. Other 3-D Structures

Numerous nondiamondoid 3-D MOFs have also been found to crystallize in noncentrosymmetric space groups, giving rise to SHG activity (Table 2). Lin et al. synthesized noncentrosymmetric 3-D MOFs of $Mn^{2+}/Co^{2+}/Ni^{2+}$ with the (4-(2-(pyridine-3-yl)vinyl)phenyl)phosphonate bridging ligand (**22**−**24**).[89] The three MOFs with different metal centers are isostructural and crystallize in the same space group *Fdd*2, showing significant SHG activities. Hong et al. used a pyridinediacrboxylalte ligand to build a 3-D MOF in the noncentrosymmetric space group $Pna2_1$ and tested its NLO properties (**25**).[90] Yao et al. used isonicotinate ligands to synthesize interpenetrated 3-D framework in the noncentrosymmetric space group $Pca2_1$ with Cu^+ nodes (**26**) and demonstrated its SHG activity.[91] They also synthesized a 3-D MOF of the pts topology using isophthalate and Zn^{2+}, which showed moderate SHG activity (**27**).[92] Chen et al. used a mixture of picolinate and isonicotinate ligands to synthesize a SHG-active 3-D MOF (**28**).[93] Zhou et al. synthesized a SHG-active 3-D Mg MOF (**29**) using benzene-1,3,5-tricarboxylate ligand with the (10,3)-a-net topology.[71] Pan et al. synthesized a new 3-D phase of zinc succinate which crystallized in chiral space group *C*2 and showed moderate SHG response (**30**).[94] Sun et al. constructed a noncentrosymmetric 3-D framework using Zn^{2+} and 4,4′-oxidiphthalate ligands (**31**).[95] These researchers also constructed a 3-D Co MOF of the noncentrosymmetric $SrAl_2$ topology using a di(imidazoly)benzoate ligand.[96] Both of these MOFs showed strong SHG responses (**32**). Liu et al. used the hydroxynicotinate ligand to synthesize a noncentrosymmetric Nd MOF with a new (3,6)-net structure, which exhibits moderate SHG activity (**33**).[97] Liu et al. synthesized a Cd 3-D MOF with a combination of bis(imidazole) and tetracarboxylate ligands and characterized its SHG property (**34**).[98] They also reacted 4,4′-sulfonyldiphthalate with Cu^{2+} and 4,4′-bipyridine as a coligand to construct 3-D MOFs with good SHG activity (**35**).[99] Wang et al. synthesized two Cd MOFs (**36** and **37**) with benzoimidazoles, which crystallize in a 3-D sqp-net and show SHG responses.[100] They also used a combination of imidazole and sulfonyldibenzoate ligands to synthesize SHG-active 3-D MOFs with Cd^{2+} and Co^{2+} (**38**−**40**).[101] Shao et al. used the *m*-BDC ligand to react with Cd^{2+} and obtained a noncentrosymmetric MOF of the pcu topology (**41**).[79] Xiong et al. used a ligand containing pyridine, imidazole, and carboxylate functionalities to construct a 3-D MOF with Mn^{2+} (**42**) that crystallizes in the noncentrosymmetric space group *Cc*.[102] Liu et al. used a combination of sulfonatoisophthalate ligand and bispyridyl ligand to synthesize a Zn MOF (**43**) in the noncentrosymmetric space group *Cc*.[103] Zhang et al. synthesized a chiral 3-D MOF using a bispyridine ligand and a Zn^{2+} connector that showed SHG activity (**44**).[104] Lu et al. synthesized a noncentrosymmetric 3-D MOF of a (3,4)-connected net based on the Cu^+ ions and a pyridinetetrazole bridging ligand (**45**).[105] Shao et al. reported the synthesis of noncentrosymmetric 3-D MOFs of the sxb topology based on the isophthalate and 5-hydroxyisophthalate bridging ligands and Cd^{2+} and Ca^{2+} ions (**46**) and of the pcu topology based on the 5-hydroxyisophthalate bridging ligand and Ca^{2+} ions (**47**).[106] Du et al. used tetrakis[4-(carboxylatostyrenyl)]methane and Zn^{2+} nodes to build 3-D interpenetrating frameworks with the sxa topology (**48**), which is SHG active. Interestingly, the two interpenetrating nets in the structure are not identical.[85] Wong et al. synthesized a 3-D coordination polymer (**49**) of Tb^{3+} and an N-tripodal ligand, crystallizing in the noncentrosymmetric space group *P*3*c*1. They observed green multiphoton upconversion and strong red (SHG) and blue (THG) NLO processes in the same system.[107]

2.4. Octupolar MOFs

The arrangement of donors and acceptors in a molecular NLO chromophore is not limited to the linear geometry (Table 3). A chromophore with 3-fold rotational symmetry, referred to as an octupolar chromophore, has been shown to exhibit better transparency/optical nonlinearity trade-off than traditional dipolar chromophores as a result of four significant components of molecular hyperpolarizability (β).[108]

Lin et al. first reported a MOF (**50**) built from a novel octupolar $[Cd_3(\mu_3\text{-}OH)L_3(py)_3]^{2+}$ building blocks with 3-fold rotational symmetry.[109] The crystal was synthesized hydrothermally from $Cd(ClO_4)_2\cdot 6H_2O$ and ethyl 4-[2-(4-pyridyl)ethenyl]benzoate under basic conditions. It adopts an infinite chiral 2-D coordination network structure based on the unsymmetrical pyridinecarboxylate connector and tricadmium octupolar nodes (Figure 15). The 2-D layers in **50** stack in a fashion to afford a chiral bulk solid (space group *R*32).

Table 2. SHG-Active MOFs with Other 3-D Framework Structures

MOFs	chemical formula	space group	folds	SHG($I^{2\omega}$)	ref
22	$Mn_2(Etpvpp)_4(H_2O)$	*Fdd*2		80 × α-quartz	89
23	$Co_2(Etpvpp)_4(H_2O)$	*Fdd*2		10 × α-quartz	89
24	$Ni_2(Etpvpp)_4(H_2O)$	*Fdd*2		70 × α-quartz	89
25	Zn(pydc)	$Pna2_1$	1	5 × KDP	90
26	$Cu_3(CN)(inic)_2$	$Pca2_1$	2	~KDP	91
27	Zn(iph)	$P4_32_12$		>KDP	92
28	[Zn(pic)(inic)]	$Pna2_1$		3.5 × KDP	93
29	$Mg_2(BTC)(CH_3COO)(DMA)_3 \cdot H_2O$	$P2_12_12_1$		5 × KDP	71
30	Zn(suc)	*C*2		6.5 × KDP	94
31	$[Zn_4(4,4'\text{-ODPA})_2(2,2'\text{-bpy})_2(H_2O)] \cdot 2H_2O$	*Cc*		0.5 × urea	95
32	$[Co(dimb)(H_2O)_2]ClO_4$	*C*2		0.4 × KDP	96
33	$Nd(Hhnic)_2(CH3COO)$	$Cmc2_1$		0.2 × KDP	97
34	$[Cd_2(bptc)(bimb)] \cdot 3H_2O$	$C222_1$		0.7 × urea	98
35	$Cu_2(SDP)(4,4'\text{-bpy})_{1.5} \cdot 2.7H_2O$	*Fdd*2		0.7 × urea	99
36	$Cd_2(imbi)_4(\mu_2\text{-Cl})Cl(H_2O)$	*P*4*nc*		3 × KDP	100
37	$Cd_2(imbi)_4(\mu_2\text{-Br})Br(H_2O)$	*P*4*nc*		2 × KDP	100
38	$Cd(SDBA)(timb) \cdot 3H_2O$	$P2_12_12_1$		0.6 × urea	101
39	Co(SDBA)(bimb)	*Cc*		0.7 × urea	101
40	Co(SDBA)(obix)	$P2_12_12_1$		0.8 × urea	101
41	$(Me_2NH_2)[CdLi(iph)_2]$	$P\bar{4}m2$		4 × KDP	79
42	Mn(HPIDC) H_2 O·$2H_2O$	*Cc*		0.8 × urea	102
43	$Zn_2(\mu_2-OH)(SIP)(dpp)$	*Cc*		2.5 × KDP	103
44	$[Zn_2(dpp)_2(bza)_2]_2 \cdot 2H_2O$	$P2_1$		active	104
45	$Cu_2(4\text{-ptz})Br$	*Cc*		3−4 × KDP	105
46	$CdCa(iph)_2(DMF)_2$	$Pna2_1$		1.5 × KDP	106
47	$CdCa(H5\text{-hiph})_2(H_2O)_2 \cdot 2Me_2NH$	$I\bar{4}c2$		2.3 × KDP	106
48	$Zn_4(tcsm)_2(H_2O)_3(DMA) \cdot 2H_2O$	*Cc*		0.6 × KDP	85
49	$Tb(tdea)(NO_3)_3$	*P*3*c*1		active	107

Table 3. SHG-Active Octupolar MOFs

MOF	chemical formula	dimension	space group	SHG($I^{2\omega}$, vs α-quartz)	ref
50	$[Cd_3(\mu_3\text{-OH})((E)\text{-4-pyv-4-bza})_3(py)_6](ClO_4)_2$	2-D	*R*32	10 × KDP	109
51a	$(H_2NMe_2)_2[Cd_3(C_2O_4)_4] \cdot$ MeOH·$2H_2O$	3-D	$I\bar{4}3d$	150	110
51b	$(NH_4)_2[Cd_3(C_2O_4)_4] \cdot$ MeOH·$2H_2O$	3-D	$I\bar{4}3d$	155	110
51c	$Na_2[Cd_3(C_2O_4)_4] \cdot$ MeOH·$2H_2O$	3-D	$I\bar{4}3d$	90	110
51d	$K_2[Cd_3(C_2O_4)_4] \cdot$ MeOH·$2H_2O$	3-D	$I\bar{4}3d$	110	110
52a	$CdCl_2(tpb) \cdot 2H_2O$	3-D	*R*32	15	111
52b	$CdBr_2(tpb) \cdot 2H_2O$	3-D	*R*32	24	111
52c	$CdI_2(tpb) \cdot 2H_2O$	3-D	*R*32	35	111
52d	$Cd(NO_3)_2(tpb) \cdot 2H_2O$	3-D	*R*32	11	111
52e	$Cd(OAc)_2(tpb) \cdot 2H_2O$	3-D	*R*32	20	111
52f	$Cd(ClO_4)_2(tpb) \cdot 2H_2O$	3-D	*R*32	17	111

Kurtz powder SHG measurements of **50** revealed a powder SHG intensity of 130 versus α-quartz.

Cui et al. recently synthesized an octupolar 3-D anionic cadmium oxalate (**51**), crystallizing in the noncentrosymmetric space group $I\bar{4}3d$. The crystals showed cation-dependent SHG responses. The as-synthesized MOF with $[H_2NMe_2]^+$ cation (**51a**) showed a SHG intensity of 150 vs α-quartz. With both 3^5S^3 and 3^4S^4 polyhedral cages in the structure, the open framework shows high ion-exchange capacities for cations NH_4^+, Na^+, and K^+. After exchanging the cations in **51a** to NH_4^+, K^+, and Na^+ (**51b**−**d**), the SHG intensity changes to 155, 90, and 110, respectively (Figure 16).[110] Cui et al. also synthesized a cationic framework of a 3-D octupolar (14,3) topology from the tris-(2,3,5,6-tetramethyl-4-(pyridine-4-yl)phenyl)borane bridging ligand and Cd^{2+} nodes. Although they used racemic ligands in the synthesis, individual crystals crystallize in the chiral *R*32 space group as a result of spontaneous self-resolution during crystallization. This MOF exhibits anion-dependent SHG responses. With Cl^-, Br^-, I^-, NO_3^-, OAc^-, and ClO_4^- anions in the MOF channels (**52a**−**f**) these materials showed powder SHG

dx.doi.org/10.1021/cr200252n |*Chem. Rev.* 2012, 112, 1084–1104

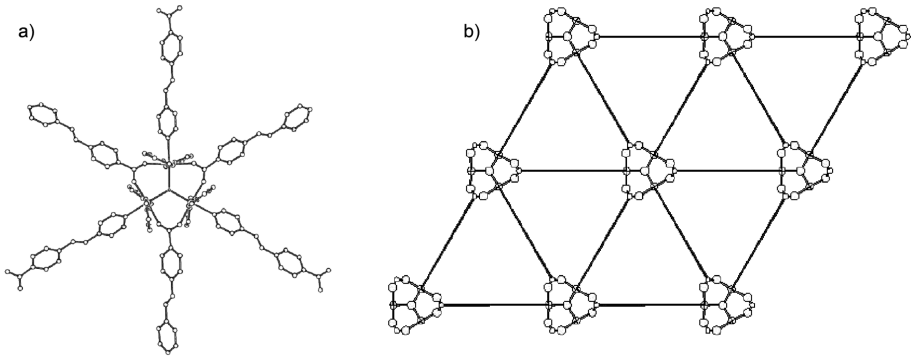

Figure 15. (a) View of the octupolar $[Cd_3(\mu_3\text{-OH})(4\text{-}[2\text{-}(4\text{-pyridyl})\text{ethenyl}]\text{benzoate})_6(py)_6]^{2+}$ building block in **50**. (b) Schematic showing the 2-D sheet in **50** down the *c* axis. Reprinted with permission from ref 109. Copyright 1999 American Chemcial Society.

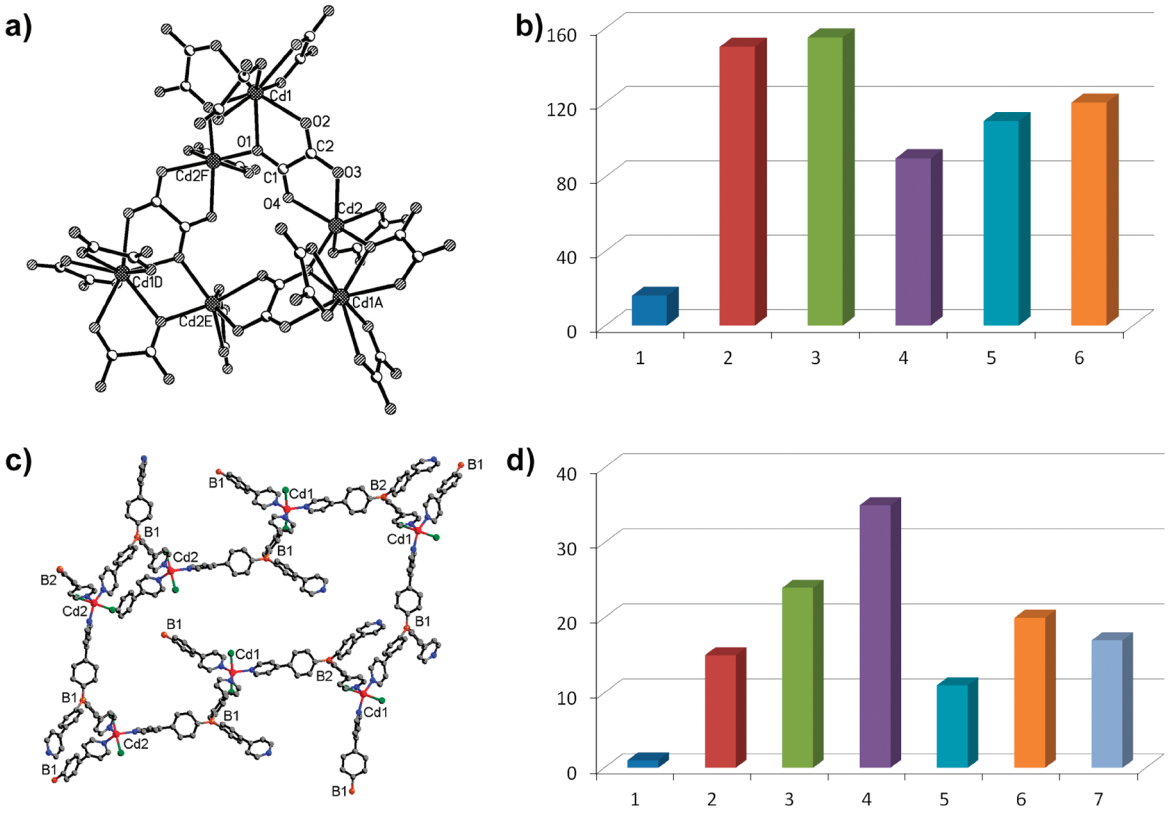

Figure 16. (a) View of the octupolar 3-D anionic open framework of **51a**. (b) Comparison of the SHG intensities of KDP, **51a**, the NH_4^+, Na^+, K^+ exchanged samples of **51b**−**51d**, and **50** (from left to right; the intensity of KDP is set as 16 vs α-quartz). (c) View of the octupolar 3-D anionic open framework of **52a**. (d) Comparison of the SHG intensities of α-quartz and the Cl^-, Br^-, I^-, NO_3^-, ^-OAc, and ClO_4^- exchanged samples of **52a**−**f** (from left to right; the intensity of α-quartz is set as 1). Reprinted with permission from refs 110 and 111. Copyright 2007 and 2008 Wiley-VCH Verlag GmbH & Co.

intensities of 15, 24, 35, 11, 20, and 17 vs α-quartz, respectively (Figure 16).[111]

2.5. Two-Dimensional Frameworks

Lin and co-workers first explored 2-D structural motifs for designing noncentrosymmetric MOFs (Table 4). They found that the bent configuration of an *m*-pyridinecarboxylate ligand can link metal centers to form 2-D square or rhombohedral grids.[22] An unsymmetrical environment is created around the d^{10} metal centers (Zn^{2+} or Cd^{2+}) when two pyridyl nitrogen and two carboxylate moieties coordinate in either a *cis*-octahedral (with chelating carboxylate groups) or a tetrahedral (with monodentate carboxylate groups) manner. The highest possible symmetry at the metal center is C_{2v}, and as a result, the metal nodes cannot possess an inversion center.

In a rhombohedral grid there are three possible positions to place the inversion centers: (1) at the corner of the rhombohedra, (2) at the middle of the edges, and (3) at the center of the rhombohedra. The unsymmetrical nature of the coordinating nodes rules out the possibility of having an inversion center at the corner of rhombohedral nets. It can be further demonstrated that the inversion centers at the edge middle point and rhombohedra

dx.doi.org/10.1021/cr200252n |*Chem. Rev.* 2012, 112, 1084–1104

Table 4. SHG-Active MOFs with 2-D Structures

MOF	chemical formula	grid	space group	SHG($I^{2\omega}$)	ref
53	$Zn(nic)_2$	square	$P4_32_12$	2 × α-quartz	112,113
54	$Zn((E)\text{-4-pyv-3-bza})_2$	square	$Fdd2$	1000 × α-quartz	112,113
56	$Zn_4((E)\text{-4-pyv-3-bza})_8 \cdot (H(E)\text{-4-pyv-3-bza}) \cdot H_2O$	rhombohedral	Cc	400 × α-quartz	113
57	$Zn((E)\text{-3-pyv-4-bza})_2 \cdot H_2O$	rhombohedral	$P2_12_12$	large	113
58	$Zn(tzpbin)_2 \cdot 1.5H_2O$	square	$Fdd2$	50 × urea	83
59	$UO_2(opyca)_2$	square	$P2_12_12_1$	0.4 × urea	114
60	$Eu(cda)_3(H_2O)_3 \cdot H_2O$	rhombohedral	Cc	16.8 × urea	115
61	$Cd_8(hnic)_8(phen)_8(H_2O)$	rhombohedral	$P2_12_12_1$	8 × KDP	116
62	$(Me_2NH_2)[Cd(H5\text{-hiph})(H_25\text{-hiph})]$ DMF · CH_3 OH · H_2O	rhombohedral	Cc	2 × KDP	79
63	$Zn_3(2,2'\text{-bpy})_3(4\text{-hiph})_2 \cdot 5H_2O$	square	$P2_1$	0.50 × urea	117
64	$Co_3(2,2'\text{-bpy})_3(4\text{-hiph})_2 \cdot 5H_2O$	square	$P2_1$	0.02 × urea	117
65	$Zn(2,6\text{-PDCO})(bbi) \cdot 0.5H_2O$	herringbone	$Pca2_1$	0.9 × urea	118
66	$Pb_3(psmp)_2Cl_2(H_2O)$	layered	Cc	1 × KDP	73
67	$Pb_3(psmp)_2Br_2(H_2O)$	layered	Cc	2 × KDP	73
68	$Zn_2(PIDC)(H_2O)Cl$	2-D	$P2_12_12_1$	1 × urea	102
69	Ag(htb)	2-D	$Pna2_1$	active	119

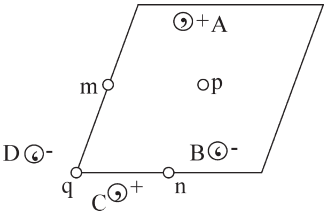

Figure 17. Schematic demonstrating the relationship among inversion centers in a rhombohedral lattice. A, B, C, and D are general points in the lattice. p, m, and q are inversion centers relating these general points. Each general point is represented by a comma/reversed-comma and ±, indicating that the point possesses internal structure (chirality).

middle are related to the inversion centers at the corners. As shown in Figure 17, if we surmise that there is an inversion center at the middle of the rhombohedron then object A can be transformed to object B by the center of symmetry (p). A and B can also be transformed to C and D by translational symmetry of the rhombohedral lattice. It is obvious that A and D as well as B and C are related by centers of symmetry at the middle of the edges (m and n), while C and D are related by a center of symmetry at the corner (q). In other words, if there are inversion centers in a rhombohedral lattice, the inversion centers should appear at the corners, the edge middles, and the rhombohedra center at the same time. With this analysis the unsymmetrical metal coordinating centers can guarantee that the 2-D rhombohedral nets do not contain any inversion centers on the plane. It is still possible for the crystal of a 2-D MOF to possess inversion centers which relate adjacent 2-D layers of different extension directions.

On the basis of this design, Lin and co-workers synthesized a series of 2-D rhombohedral or square networks with Zn^{2+}/Cd^{2+} metal nodes and systematically elongated *m*-pyridinecarboxylate linkages through hydro(solvo)thermal synthesis (Figure 18). Four of these 2-D MOFs crystallize in noncentrosymmetric space groups.[112,113]

The Zn centers in $Zn(nic)_2$, **53**, coordinate to two bidentate carboxylate groups and two pyridyl nitrogen atoms in a cis configuration, leading to a distorted octahedral geometry. These octahedral Zn centers are then linked by the bent nicotinate ligands to form a chiral infinite rhombohedral grid. Individual grids stack via the 4_3 axis to form the bulk solid crystallizing in chiral space group $P4_32_12$ (Figure 19).

Similar to the diamondoid structures, as the ligand length and void space within the grid increases, individual grids can then interweave to fill the void space and thus to enhance structural stability. As an example, in $Cd[(E)\text{-4-pyv-3-bza}]_2$, **54**, the void space resulting from a long bridging ligand is effectively reduced by 3-fold interweaving. Similar to that observed in the diamondoid frameworks, an odd-number-fold interweaving retains the chirality of individual net (Figure 20). **54** thus crystallizes in the noncentrosymmetric $Fdd2$ space group. On the other hand, an even-number-fold interweaving can bring an inversion center to lead to a centrosymmetric solid, as illustrated by the synthesis of $Zn[(E)\text{-3-pyv-5-tpa}]_2$, **55** (Figure 21).[113] The two interweaved 2-D rhombohedral nets in **55** are crystallographically related by a center of inversion, leading to a centrosymmetric solid in space group *Pcca*.

Noncentrosymmetric solids can still form from 2-D networks with an even-number-fold interweaving. $Zn_4[(E)\text{-4-pyv-3-bza}]_8 \cdot [H(E)\text{-4-pyv-3-bza}] \cdot (H_2O)$, **56**, for example, was built from stacking four independent 2-D grids in an *ABC*-type sequence (Figure 22).[113] The presence of a 2-fold interweaving in the *A* sequence nets does not prevent the bulk solid from crystallizing in the noncentrosymmetric space group *Cc*.

As mentioned above, an inversion center can result from stacking the 2-D networks along the third dimension. Although less control can be exerted through weak noncovalent interactions in stacking 2-D networks, certain packing arrangements do inhibit the occurrence of centrosymmetry. The pleated sheet topology is one of them that disfavors a centrosymmetric packing. In $Zn[(E)\text{-3-pyv-4-bza}]_2 \cdot (H_2O)$, **57**, a highly distorted rhombohedral 2-D grid structure is formed as a result of the low coordination number of the Zn centers.[113] Adjacent rows of Zn centers within each 2-D grid are found to be offset by 2.93 Å along the *c* axis (Figure 23). The pleated 2-D grids effectively induce tooth-fitting-type packing between adjacent layers, avoiding formation of a centrosymmetric bulk solid. As a result, **57**

dx.doi.org/10.1021/cr200252n |*Chem. Rev.* 2012, 112, 1084–1104

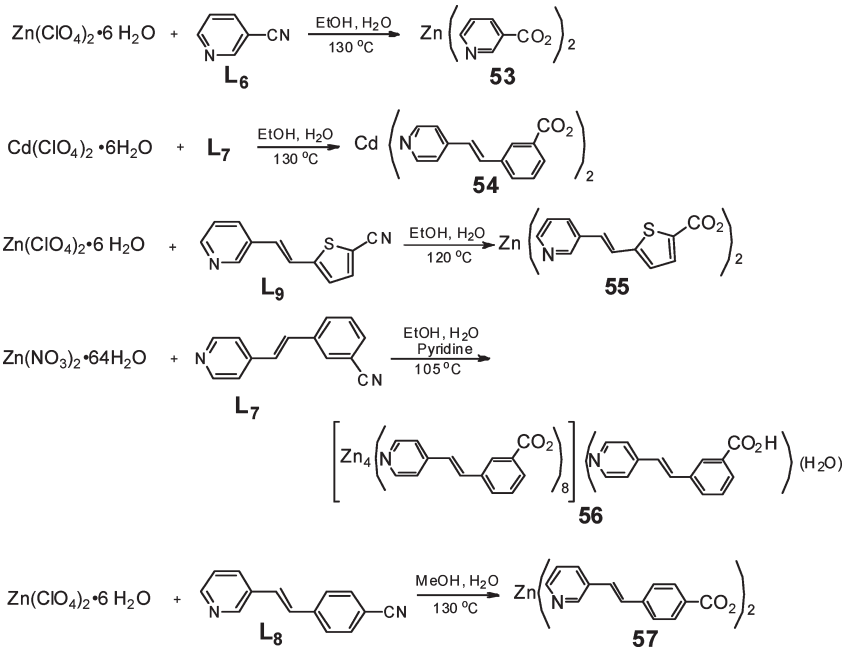

Figure 18. Synthesis of 2-D MOFs based on d^{10} metal connecting points and bent *m*-pyridinecarboxylate bridging ligands. Reprinted with permission from ref 113. Copyright 2001 American Chemical Society.

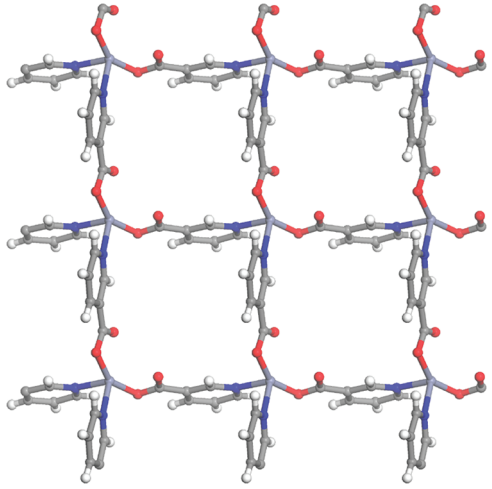

Figure 19. Two-dimensional square grid structure of **53**.

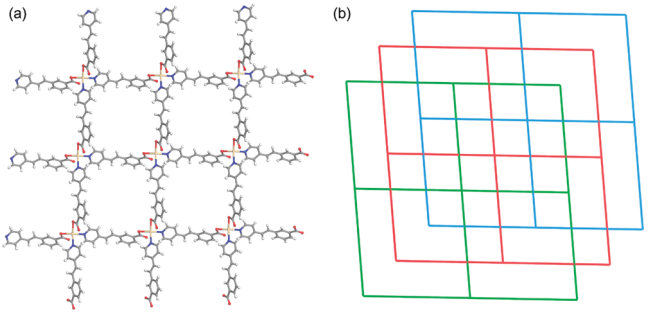

Figure 20. (a) View of the 2-D rhombohedral grid structure of **54** showing the presence of large void space. (b) Schematic showing the interweaving of three independent rhombohedral grids in the *ac* plane in **54**.

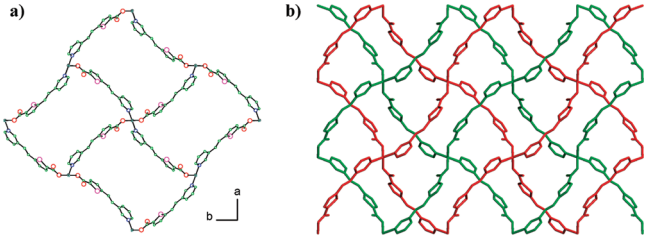

Figure 21. (a) Two-dimensional square grid structure of **55**. (b) Two-fold interweaving of the 2-D grids in **55**. The two networks are related by an inversion center. Reprinted with permission from ref 113. Copyright 2001 American Chemical Society.

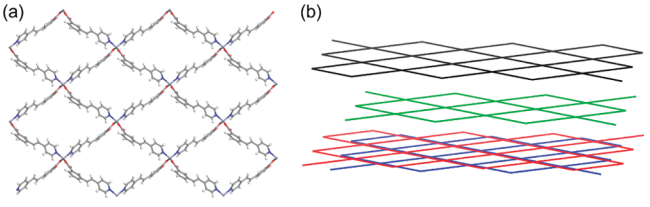

Figure 22. (a) Two-dimensional rhombohedral grid in **56**. (b) Stacking of four independent 2-D rhombohedral grids along the *c* axis.

crystallizes in the chiral space group $P2_12_12$. All these noncentrosymmetric MOFs with 2-D grid structures are SHG active. Crystals of **54** exhibit higher SHG intensity than technologically important $LiNbO_3$.

A number of other research groups have also synthesized noncentrosymmetric MOFs based on similar 2-D grid designs. Xiong et al. obtained a zinc MOF (**58**) built from in-situ-generated substituted, unsymmetrical tetrazole ligand under solvothermal conditions. **58** shows very large SHG responses.[83] The Zn centers adopt a distorted tetrahedral environment by

coordinating to two pyridyl groups and two tetrazole groups. The 2-D framework crystallizes in the noncentrosymmetric space group *Fdd*2 (Figure 24). The authors also used UO_2^+ as the metal connector to build a noncentrosymmetric 2-D square network (**59**) with the 1-oxo-4-pyridylcarboxylate bridging ligand.[114] Shi et al. used the carbonyldicyanomethanide anion to construct a rhombohedral grid with Eu^{3+} (**60**) that showed impressive SHG activity.[115] Feng et al.,[116] Du et al.,[79] and Chen et al.[117] used hydroxynicotinate or hydroxyisophthalate to construct square or rhombohedral nets with Cd^{2+}, Zn^{2+}, or Co^{2+}, which showed moderate SHG responses (**61**−**64**).

Two-dimensional grids with other motifs have also been reported in the literature to be SHG active. Meng et al. synthesized a noncenterosymmetric 2-D framework of a herringbone pattern which is SHG active (**65**).[118] Xie et al.[73] constructed layered organophosphonates with Pb^{2+} ions (**66** and **67**). The phosphonates are oriented perpendicular to the 2-D layers to lead to noncentrosymmetric crystal structures which show moderate SHG activities. Xiong et al. used the pyridinecarboxylate ligand to react with Zn^{2+} ions to obtain a chiral 2-D framework containing both tetrahedral and octahedral Zn^{2+} centers, crystallizing in the $P2_12_12_1$ space group (**68**).[102] Janiak et al. used the poly(pyrazolyl)borate ligand and Ag^+ ion to construct a 2-D structure (**69**) with a tetrahedral coordination environment around the Ag^+ center. They also experimentally determined one element of the $\chi^{(2)}$ tensor.[119]

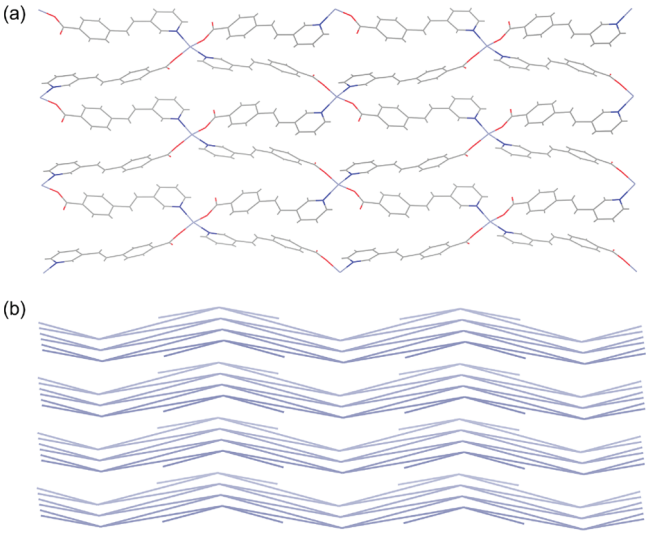

Figure 23. (a) Two-dimensional rhombohedral grid of **57**. (b) Stacking of adjacent 2-D pleated sheets in **57**.

2.6. One-Dimensional Chains and Other Related Helical Structures

Noncentrosymmetric or chiral 1-D helical metal−organic chains have been widely reported in the literature (Table 5), but it is much more difficult to systematically design noncentrosymmetric bulk solids based on 1-D chains than 3-D or 2-D structural motifs. The 1-D chain systems lack control in two other directions.

Lin et al. first synthesized a noncentrosymmetric 1-D coordination polymer (**70**) using 3-(4-(2-(pyridine-4-yl)vinyl)phenyl)-acrylate and Zn^{2+} nodes.[120] The Zn centers are connected through the bridging ligands to form a 1-D zigzag chain, with pyridyl groups not coordinating to metal centers (Figure 25). These 1-D chains are running along mutually perpendicular directions, and $\pi-\pi$ interactions play a significant role in organizing the 1-D chains into the 3-D structure with open channels of ~4.6 × 11.8 Å along the *c* axis. As shown in Figure 25, the polar axis of **70** lies along the *c* axis with all dipoles canceling each other along both the *a* and the *b* axes. **70** exhibits a powder SHG intensity of 75 vs α-quartz.

Many other noncentrosymmetric solids based on 1-D chain structures have been reported. Xiong et al. used a similar 3-(2-(pyridine-2-yl)vinyl)benzoate ligand to construct the 1-D chain (**71**), showing SHG responses comparable to that of urea.[121,122] Yao et al. recently developed 1-D SHG-active materials based on coordination polymers of phthalate and Zn^{2+} with 1,3-di(pyridine-4-yl)propane as a coligand (**72**).[122] Liu et al.[101] and Zheng et al.[104] used a combination of dicarboxylate ligands and bisimidazoles to react with Zn^{2+} and Cd^{2+} to form SHG-active chiral helical chains (**73** and **74**). Liu et al. synthesized a chiral 1-D chain (**75**) using Cu^{2+} and 4,4′-(perfluoropropane-2,2-diyl)diphathalte, which is decorated by carboxylate moieties and further packed to a 3-D structure by a hydrogen bond.

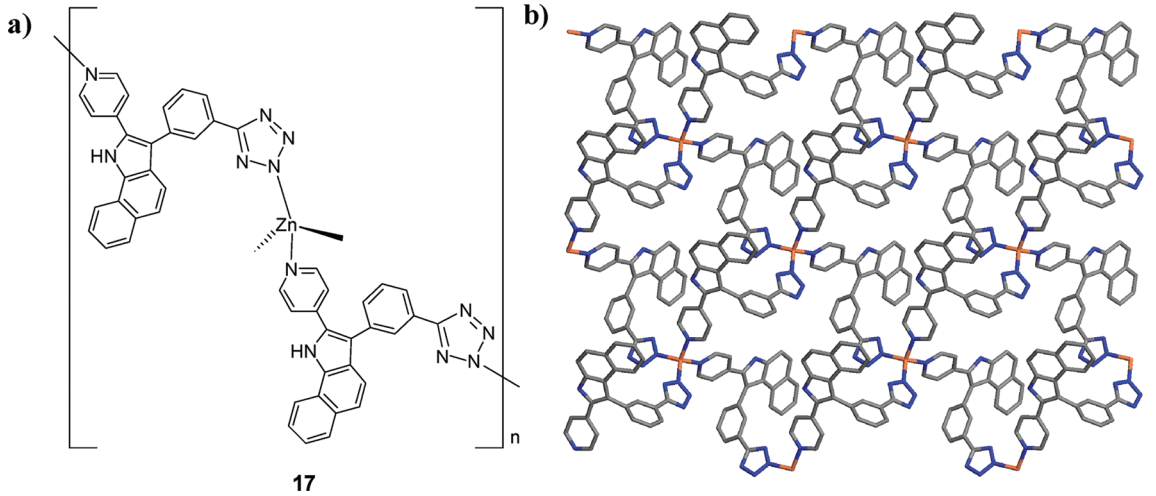

17

Figure 24. (a) Chemical structure of **58**. (b) View of the 2-D grid structure of **58**. Reprinted with permission from ref 83. Copyright 2005 American Chemical Society.

Table 5. SHG-Active MOFs with 1-D Chain and Related Structures

MOF	chemical formula	dimension	space group	SHG($I^{2\omega}$)	ref
70	$[Zn(pec)(H_2O)]\cdot CH_3\,CN\cdot 3H_2O$	1-D	*Fdd*2	75 × α-quartz	120
71	$Zn((E)\text{-2-pyv-3-bza})_2$	1-D	$P2_12_12_1$	1 × urea	121
72	$Zn_2(dpp)(pht)_2$	1-D	*Cc*	2 × KDP	122
73	$Zn_2(SDP)(bimb)$	1-D	$P2_12_12_1$	0.7 × urea	101
74	$Zn(dpp)(bza)_2\cdot 2H_2O$	1-D	*Aba*2	active	104
75	$Cu(H_2FA)(2,2'\text{-bpy})\cdot 1.54(H_2O)$	1-D	$P2_12_12_1$	0.8 × urea	99
76	$CdI_2(ppodz)$	1-D	$P2_1$	0.4 × KDP	123
77	$CdI_2(ppodz)(H_2O)\cdot 2DMF$	1-D	$P2_12_12_1$	0.5 × KDP	123
78	$Zn(BTA)_2H_2O$	1-D	*Cc*	1 × KDP	124
79	$DyCl_3(dicnq)_2$	1-D	$P2_1$	2 × KDP	125
80	$(Me_2NH_2)[Cd_3(H_2O)_3(OH)(SDBA)_3]$	1-D	*P*3	<KDP	79
81	$[Zn(pyz)(H_2O)_4]\,[pht]$	1-D	*Imm*2	3 × KDP	126
82	$CuI_3(pymt)_3$	1-D	$P2_12_12_1$	<KDP	127
83	$Cd_2(DPA)_2(mbix)$	1-D	$P6_1$	0.7 × urea	128
84	$Zn(2,6\text{-PDCO})(H_2O)_2$	1-D	$I4_1cd$	0.3 × urea	118
85	$[(18\text{-crown-6})K][Cd(SCN)_3]$	1-D	$Cmc2_1$	200× α-quartz	129
87	$[Et_4N][Cd(SCN)_3]$	1-D	$Cmc2_1$	weak	130
88	$[Et_4N][Cd(SeCN)_3]$	1-D	$Cmc2_1$	weak	130
89	$[Me_4N][Cd(SCN)_3]$	1-D	$Pna2_1$	weak	130
90	$[Me_4N][Cd(SeCN)_3]$	1-D	$Pna2_1$	weak	130
91	$[Zn(pyz)(H_2O)_2]MoO_2F_4$	1-D	$P3_1/P3_2$		131
92	$Zn_2(2,6\text{-PDCO})_2(4,4'\text{-bpy})_2(H_2O)_2\cdot 3H_2O$	2-D	$P2_1$	0.3 × urea	118
93	$Cu(2,3\text{-PDCO})(4,4'\text{-bpy})\cdot H_2O$	2-D	*C*2	0.6 × urea	133
94	$Zn(2,3\text{-PDCO})(bix)\cdot H_2O$	2-D	$P2_1$	0.8 × urea	133
95	$Zn_2(3,3'\text{-ODPA})(4,4'\text{-bpy})(H_2O)_3\cdot 2H_2O$	2-D	$P2_12_12_1$	0.8 × urea	132
96	$Cd(SDBA)(bimb)$	2-D	$P2_1$	0.8 × urea	128
97	$Zn(ptmb)(OH)$	2-D	$P2_1$	5 × KDP	134
98	$[Cd(pic)(inic)(H_2O)]\cdot N_2H_4$	2-D	$P2_1$	1.5 × KDP	93
99	$Zn(OH)(3\text{-ptz})$	2-D	*Fdd*2	active	135
100	$Zn((Z)\text{-3-pyv-4-bza})_2\cdot 0.5H_2O$	3-D	*P*32	6 × α-quartz	136
101	$Cd_{2.5}(pec)_5\cdot EtOH\cdot 5H_2O$	3-D	*Fdd*2	20 × α-quartz	120
102	$Cd(N_3)(3\text{-ptz})$	3-D	$P3_121$	active	135
103	$ZnCl(4\text{-ptz})$	3-D	*Pc*	active	135
104	$Zn(apa)(ClO_4)$	3-D	$P2_12_12_1$	active	87
105	$(Hpy)_2[In_2(BTC)_2(\mu\text{-}OH)_2]$	3-D	$P2_1$	3 × KDP	72
106	$Cd(AmTAZ)Cl$	3-D	$P2_12_12_1$	<KDP	137
107	$Cd_2(3,3'\text{-ODPA})(4,4'\text{-bpy})(H_2O)_3\cdot(H_2O)_2$	3-D	$P2_1$	1 × urea	132
108	$Zn(OH)(quin\text{-}6\text{-}c)$	3-D	$Pna2_1$	460 × α-quartz	138
109	$Cd(trtr)_2$	3-D	*Fdd*2	6 × KDP	139
110	$[Zn_2(tcom)(H_2O)]_2\cdot 3H_2O$	3-D	*Fdd*2	1.5 × KDP	140
111	$Cd_3(datrz)_6(H_2O)_2$	3-D	*C*2	0.2 × KDP	141
112	$Ni(Hpdc)(bth)(H_2O)$	3-D	$P2_12_12_1$	0.3 × urea	142
113	$Zn(Hbtc)(ddm)$	3-D	$P2_12_12_1$	4 × KDP	143

77 shows an SHG signal of 0.8 times of the urea standard.[99] Wang employed ligands with pyridine, diazole, or triazole and carboxylate coordinating groups to obtain three chiral 1-D MOFs with Cd^{2+} or Zn^{2+} (**76**−**78**), which showed weak SHG responses.[123,124] Guo et al. synthesized an SHG-active chiral chain from Dy^{3+} and a dipyridoquinoxaline ligand (**79**).[125]

Nonchiral chains can also crystallize in noncentrosymmetric space groups, giving rise to SHG activities (**80**−**84**).[79,118,126−128] Counterions in the structure can also be used to induce noncentrosymmetric packing of 1-D chains. Teo et al. first synthesized polymeric cadmium chacogenocyanates.[129,130] The intrinsically noncentrosymmetric anionic $[Cd(XCN)_3^-]_\infty$ (X = S or Se) chains can be assembled in either centrosymmetric or noncentrosymmetric space groups, depending on the symmetry of the cations (Figure 26). For example, the centrosymmetric dimeric $[(18\text{-crown-6})_2Na_2(H_2O)_2]^{2+}$ leads to a centrosymmetric space group $P2_1/n$ (**85**). In contrast, the noncentrosymmetric monomeric cation $[(18\text{-crown-6})K]^+$ favors formation of a noncentrosymmetric structure (**86**). Similarly, the tetraalkylammonium cations in **87**−**90** do not possess inversion centers, and as a result, **87**−**90** all crystallize in noncentrosymmetric space groups.

dx.doi.org/10.1021/cr200252n |*Chem. Rev.* 2012, 112, 1084–1104

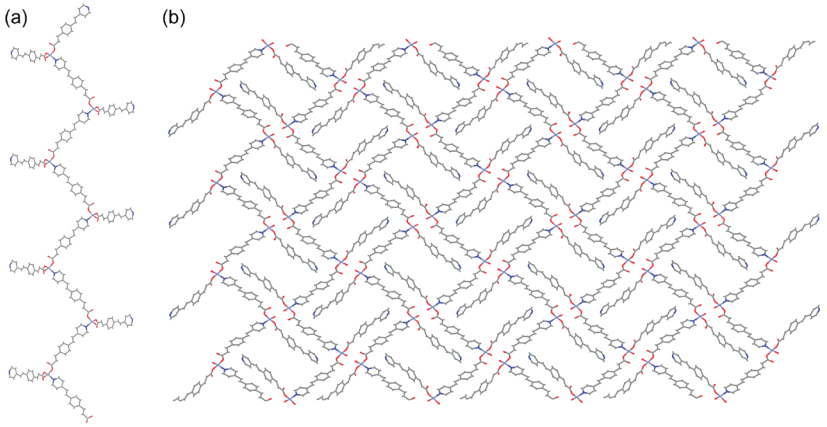

Figure 25. (a) View of the 1-D zigzag chain in **70**. (b) View of **70** down the *c* axis. Interdigitation via edge-to-face $\pi-\pi$ interactions is clearly visible.

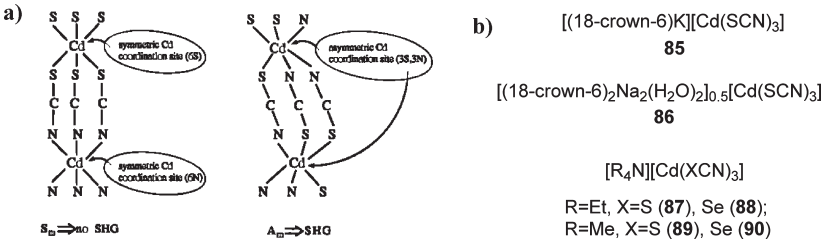

Figure 26. (a) Schematic representation of centrosymmetric and noncentrosymmetric $[Cd(SCN)_3^-]_\infty$ chains. (b) Chemical formulas of compounds **85**−**90**. Reprinted with permission from ref 130. Copyright 1999 Elsevier.

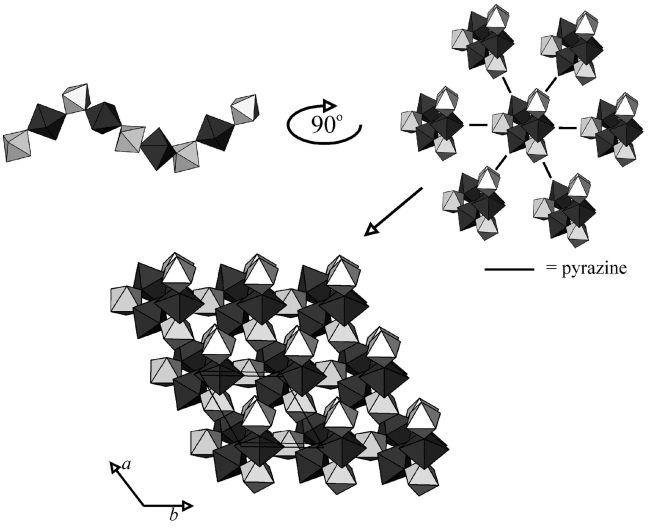

Figure 27. Polyhedral presentation of a helical chain of **91** and the linking of neighboring helices to form a chiral solid. Reprinted with permission from ref 131. Coryright 2001 American Chemical Society.

Noncentrosymmetric structures of 1-D anionic transition metal oxyfluoride chain $[MoO_2F_4^{2-}]_\infty$ were prepared by Poeppelmeier et al. (Figure 27).[131] Although the $[MoO_2F_4^{2-}]_\infty$ chain is intrinsically noncentrosymmetric as a result of the distorted octahedral coordination environment, the orientational disorder of the oxyfluoride anions often leads to centrosymmetric structures. Poeppelmeier et al. discovered that cocrystallization with certain cations can help to orient the $[MoO_2F_4^{2-}]_\infty$ anions in an ordered manner to effectively reduce the local symmetry and to promote formation of noncentrosymmetric structures. $[Zn(pyrazine)_2(H_2O)_2]^{2+}$ was used as the countercation in **91**, which leads to a 1-D structure crystallizing in a pair of enantiomorphous chiral space groups $P3_1$ and $P3_2$.

In some cases, helical chains can further interlink with each other to form 2-D and 3-D structures. Although formation of these kinds of noncentrosymmetric 2-D or 3-D structures is more of an observation than rational control, a number of examples have been reported in the literature.

Meng et al. used a combination of pyridinecarboxylate and bipyridine ligands to build chiral 2-D frameworks with Zn^{2+} and Cu^{2+} ions that are constructed from helical chains (**92**−**95**), leading to SHG activity.[118,132,133] Liu et al.[128] used pyridine−imidazole ligands and Zn^{2+}/Cd^{2+} ions to synthesize 2-D MOFs in noncentrosymmetric space groups with high SHG activities (**96**). The frameworks can be best visualized as interlinked 1-D chiral chains. Hong et al.[134] and Wang et al.[93] also built chiral 2-D framework structures from interconnected helical chains using pyridinecarboxylate ligands and Zn^{2+}/Cd^{2+} ions that are SHG active (**97** and **98**). Xiong also obtained a 2-D structure containing helical chains that were built from Zn^{2+} ions and tetrazole ligands (**99**).[135]

Lin et al. used the helical chains built from (*Z*)-4-(2-(pyriin-3-yl)vinyl)benzoate ligand (*Z*-3-pyv-4-bza) and (*E*)-3-(4-(4-((*E*)-2-pyridin-4-yl)vinyl)phenyl)acrylate and Zn^{2+}/Cd^{2+} nodes to form noncentrosymmetric 3-D solids (**100** and **101**).[120,136] In $Zn(Z\text{-3-pyv-4-bza})_2\cdot 0.5H_2O$, **100**, for example, the staggered bridging ligand induces formation of 6-fold helices.[136] Neighboring helices of **100** have the same handedness and are covalently bridged by pyridylethenylbenzoate ligands to result in a chiral

dx.doi.org/10.1021/cr200252n |*Chem. Rev.* 2012, 112, 1084–1104

3-D MOF (Figure 28). **100** exhibits a modest powder SHG efficiency of 6 times that of α-quartz.

Several examples of interlocking of 1-D chiral chains into 3-D noncentrosymmetric structures have also appeared in the literature. Xiong et al. constructed noncentrosymmetric 3-D framework from zigzag chains or strips using a pyridinetetrazole ligand and Cd^{2+}/Zn^{2+} ions (**102**−**104**).[87,135] Hong et al. used benzene-1,3,5-tricarboxylate ligand to react with In^{3+} to form 1-D chiral "tunnels", which are further linked into 3-D frameworks (**105**).[72] A chiral 3-D structure built from 1-D helical chains was constructed from the 3-amino-1,2,4-triazole ligand and the Cd^{2+} node by Zhang et al., which showed SHG activity (**106**).[137] Meng et al. obtained a 3-D Cd MOF (**107**) that was built from helical chains with oxyldiphthalate and bipyridine bridging ligands. **107** showed SHG activity that is comparable to the urea standard.[132] Liang et al. used a quinolinecarboxylate ligand to synthesize a highly SHG-active 3-D MOF (**108**) that was built from helices.[138]

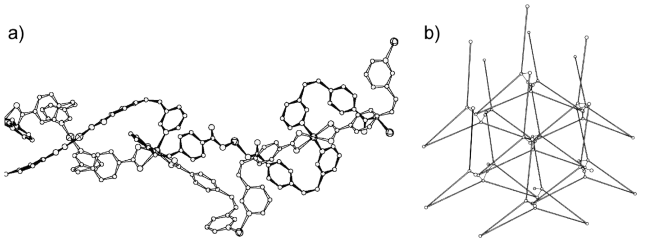

Figure 28. (a) View of the cross-link between a primary and a secondary helix in **100**. (b) Perspective view of **100** slightly away from the *c* axis showing the 3-D network resulting from the cross-linking of primary and secondary helices. Only Zn atoms are shown. Reprinted with permission rom ref 136. Copyright 2006 The Royal Society of Chemistry.

Guo et al. constructed a 3-D MOF (**109**) using bis(triazole) ligands and Cd^{2+} ions. **109** is built from interconnected 1-D helical chains and is SHG active.[139] Cao et al. obtained a noncentrosymmetric 3-D MOF (**110**) from Cd^{2+} ions and tetracarboxylate ligands. **110** is built from helical chains and shows moderate SHG signals.[140] Yao et al. used 3,5-diamino-1,2,4-triazole ligand to construct chiral chains with Cd^{2+} ions which are further connected to form a 3-D framework (**111**).[141] Zuo et al. used a combination of a pyrazolecarboxylate group and a pyridinetetrazole group to construct a chiral 3-D MOF (**112**) that forms from 1-D chiral chains.[142] Dai et al. synthesized a Zn 3-D chiral framework (**113**) with a combination of tricarboxylate and dianiline ligands. **113** is constructed from helical chains and shows modest SHG activity.[143]

2.7. MOFs Built from Chiral Ligands

The symmetry requirement for SHG activity is the absence of an inversion center. As crystals in chiral space groups necessarily lack inversion centers, all chiral crystals are in principle SHG active. If enantiopure ligands are used in MOF synthesis, the resulting MOF crystals must crystallize in chiral space groups, as long as the ligands do not racemize under the reaction conditions. Building chiral MOFs with enantiopure ligands appears to be the most straightforward strategy to design SHG-active materials (Table 6). However, chiral MOF structures do not necessarily orient the dipoles of chromophoric building blocks in a noncentrosymmetric fashion. As a result, chiral MOFs built from enantiopure ligands do not necessarily exhibit impressive SHG responses.

Radhakrishnan et al. used enantiopure *N*,*N*′-bis(4-cyanophenyl)-(1*R*,2*R*)-diaminocyclohexane (BCDC) ligand to construct 1-D and 2-D coordination polymers **114** and **115** with Ag^+ and Cu^+ nodes (Figure 3).[144,145] Crystals of **114** were grown

Table 6. SHG-Active Chiral MOFs Built from Chiral Ligand

MOF	chemical formula	dimension	ligand used	space group	SHG($I^{2\omega}$)	ref
114	[Ag(BCDC)]ClO4	1-D	homochiral	$P2_12_12_1$	2.9 × urea	145
115	[Cu(BCDC)]PF_6·THF	2-D	homochiral	$P22_12_1$	0.2 × urea	144,145
116	[Zn(bddp)·$(H_2O)_4]_2$·H_2O	1-D	homochiral	$P2_1$	0.6 × urea	146
117	$Cu_2(phen)_2(tart)(H_2O)$·$8H_2O$	1-D	homochiral	$P2_1$	0.8 × KDP	147
118	Cu(phen)(H_2tart)·$6H_2O$	1-D	homochiral	$P2_12_12_1$	0.9 × KDP	147
119	Cd(D-ca)(bte)·H_2O	2-D	homochiral	*Aba*2	0.3 × urea	148
120	Cd_4(D-ca)$_4$(btp)$_2$(H_2O)$_4$	3-D	homochiral	$P2_1$	0.8 × urea	148
121	Cd(D-Hca)$_2$(bth)(H_2O)·H_2O	3-D	homochiral	*P*1	0.4 × urea	148
122	Zn(tpcc)$_2$(H_2O)$_2$	2-D	homochiral	*C*2	2.8 × KDP	149
123	Cd(tpcc)$_2$(H_2O)$_2$	2-D	homochiral	*C*2	2.6 × KDP	149
124	Mn(H_2O)(SCMC)	3-D	homochiral	$P2_1$	active	150
125	Zn(SCMC)(H_2O)	2-D	homochiral	$P2_1$	0.05 × urea	151
126	Cd(SCMC)(H_2O) ·$2H_2O$	2-D	homochiral	$P2_12_12_1$	0.06 × urea	151
127	Zn(lac)(inic)	2-D	homochiral	$P2_12_12_1$	1.2 × urea	152
128	UO_2(lac)$_2$	2-D	homochiral	$P2_1$	0.1 × urea	114
129	Zn(SPA)(H_2O)$_2$	1-D	homochiral	$P2_12_12_1$	1 × urea	153
130	Mn(Hdnty)$_2$	2-D	homochiral	$P2_12_12$	6 × urea	154
131	Nd(Hdnty)$_2$(NO_3)(H_2O)$_5$·$3H_2O$	3-D	homochiral	$P2_1$	5 × urea	154
132	(NH_4)[Zn(hpac)]	3-D	racemic	$Pna2_1$	0.8 × KDP	155
133	Cd(eimnic)$_2$	3-D	racemic	*Fdd*2	20 × KDP	156
134	Zn(app)(NO_3)	3-D	racemic	$P2_12_12_1$	active	87
135	[Cd(app)(Happ)]ClO_4·H_2O	3-D	racemic	*Cc*	active	87
136	Cd(pdbpt)$_2$(H_2O)$_2$	1-D	racemic	*Cc*	80 × urea	157

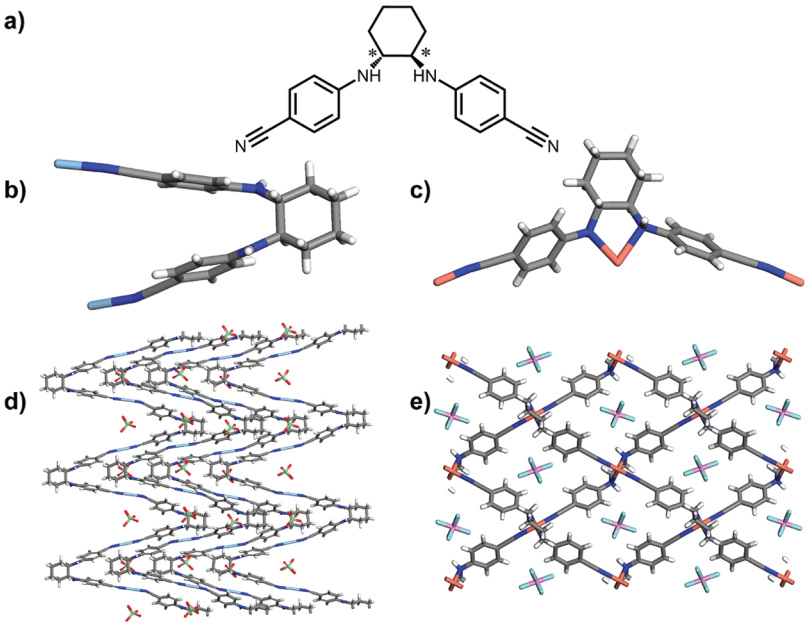

Figure 29. (a) Structure the chiral ligand used in MOF synthesis. (b) Ligand with the exo configuration in the crystal structure of **114**. (c) Ligand with the endo configuration in the crystal structure of **115**. (d) Crystal structure of **114**. (e) Crystal structure of **115**.

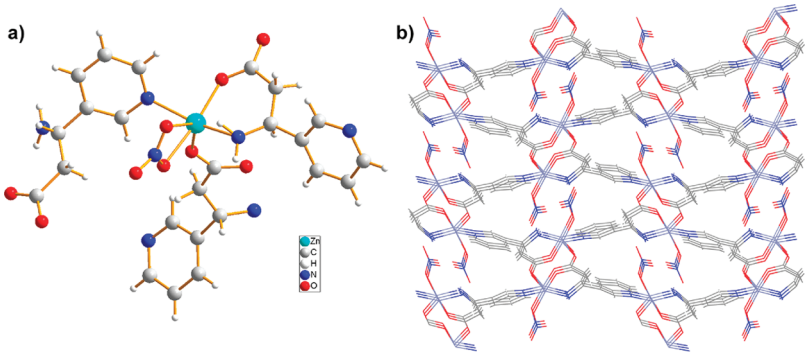

Figure 30. (a) Coordination environment of Zn^{2+} ion in **132**. (b) Crystal structure of **132**.

by slow evaporation of acetonitrile solution of BCDC and $AgClO_4$ mixture, Figure 29. In **114**, two cyano groups coordinate to one Ag^+ ion in a linear fashion to form a 1-D helical chain with the BCDC ligands oriented in an endo configuration. In contrast, reaction of BCDC and $[Cu(CH_3CN)_4]PF_6$ in dichloromethane gives a crystal of **115** with a rhomboheral 2-D network structure. The Cu^+ ions reside on a 2-fold axis in the crystal structure ($P22_12_1$ space group) and adopt a tetrahedral environment by coordinating to two amino groups of a BCDC ligand and cyano groups of two other BCDC ligands. As a result, the BCDC ligand adopts an exo configuration in the crystal structure of **115**. SHG measurements showed that **114** and **115** possessed SHG intensities of 2.9 and 0.2 times the urea standard, respectively. The authors attributed the difference of SHG activity mainly to the different configurations of the BCDC ligand in the crystal. Following this strategy, You et al. linked the (2*R*,2′*R*)-2,2′-terephthaloylbis(azanediyl)dipropanoate ligand with Zn^{2+} ions to synthesize 1-D chiral coordination polymer (**116**) that is SHG active.[146]

Enantiopure chiral ligands can be readily derived from amino acids or other natural products. Mostafa et al. used tartrate ligand to coordinate with Cu^{2+} to construct chiral 1-D helix chains, which are weakly SHG active (**117** and **118**).[147] Zuo et al. used a chiral D-camphoric acid ligand together with bis(triazole) as coligands to form chiral structures **119**−**121** with Cd^{2+},[148] all of which are SHG active. Chen et al. synthesized (1*R*,3*S*)-1,2,2-trimethyl-3-(pyridine-4-ylcarbomoyl)cyclopentanecarboxylic acid from D-camphoric acid and used the chiral ligand to grow Zn and Cd MOFs **122** and **123** that showed good SHG activity.[149] Zheng et al.[150] and Wang et al.[151] used *S*-carboxymethyl-*L*-cysteine to build chiral crystals **124** with Mn^{2+} and **125**/**126** with Zn^{2+} and Cd^{2+} for SHG applications. Xiong et al. used *S*-(−)-lactate together with the isonicotinate coligand to coordinate to Zn^{2+} and UO_2^+ ions, leading to formation of SHG-active, chiral MOFs **127** and **128**. They also used 4-sulfo-L-phenlalanine to link Zn^{2+} ions to form 1-D chiral chains **129** and used 3,5-dinitrotyrosine to synthesize Mn^{2+} and Nd^{3+} MOFs (**130** and **131**) with impressive SHG activities.[152−154]

Noncentrosymmetric MOFs can also be constructed from racemic ligands which can be much more readily available than the corresponding enantiopure ligands. When racemic ligands

dx.doi.org/10.1021/cr200252n |*Chem. Rev.* 2012, 112, 1084–1104

are used in MOF synthesis, two possibilities can be anticipated: (1) the two enantiomers crystallize in the same crystal structure in either a random or an ordered manner, leading to "meso" crystals, and (2) one enantiomer exclusively crystallizes in one crystal, a process often referred to as self-resolution. The former scenario does not orient the chromophoric units into a noncentrosymmetric arrangement and is not of interest to NLO material design. The latter situation affords noncentrosymmetric arrangements of the chromophores even though the vast majority of bulk samples from self-resolution processes contain a racemic mixture of chiral MOF crystals. Such nonchiral and noncentrosymmetric MOFs can be used in SHG.

Xiong et al. used racemic 3-amino-3-(pyridine-3-yl)propanoate (app) and Zn^{2+} ions to construct a SHG-active MOF (**132**, Figure 30) by taking advantage of the self-resolution process (Figure 4).[87] Each Zn center in the structure coordinates to three app ligands and a monodentate nitrate anion in a 5-coordination fashion, leading to formation of the (10,3)-a framework topology in the chiral space group of $P2_12_12_1$. The bulk sample of **132** is however a racemic mixture of chiral MOFs. Although numerous attempts have been made to prepare SHG-active MOFs based on the self-resolution strategy, the majority of these efforts yielded meso-MOFs. Only a small number of these MOFs crystallize in noncentrosymmetric space groups and were shown to exhibit SHG activities (**133**−**136**).[87,155−157]

3. CONCLUDING REMARKS

We surveyed the design and synthesis of a new class of second-order NLO materials based on metal−organic frameworks. The ability to rationally design noncentrosymmetric MOFs by taking advantage of the strong and highly directional nature of metal−ligand coordination bonds differentiate this class of materials from all previous systems (including traditional inorganic materials, organic crystals, inclusion compounds, poled polymers, LB films, and self-assembled chromophoric supperlattices). By judiciously choosing metal nodes and bridging ligands, the metal−ligand coordination bonds can be used to counteract the typically centric dipole−dipole interactions to lead to noncentrosymmetric MOFs.

Among all the MOF topologies explored, 3-D diamondoid networks represent the most reliable and predictable topology for the crystal engineering of noncentrosymmetric solids. A series of SHG-active MOFs of the diamondoid topology were synthesized with systematically elongated unsymmetrical linear ligands in combination with optically transparent Zn^{2+} and Cd^{2+} ions. The relationship between framework interpenetration and bridging ligand length was also delineated. With the 3-D diamondoid networks, researchers have effectively reduced a very daunting task of crystal engineering a noncentrosymmetric solid to a very simple choice of bridging ligand of appropriate length.

A number of noncentrosymmetric 3-D structures of other topologies have also been synthesized, albeit with much less control and predictability. Noncentrosymmetric octupolar MOFs which have 3-fold rotation symmetry are also explored, representing an interesting class of interesting NLO materials owing to their improved transparency/optical nonlinearity trade off as a result of the presence of four significant components of molecular hyperpolarizability.

Rhombohedral 2-D nets provide another platform for systematic design of noncentrosymmetric crystals. However, centrosymmetry can arise either from even-number fold interweaving (interlocking) or from centrosymmetric stacking of the 2-D grids. Pleated sheets can effectively prevent centrosymmetric assembly of the 2-D networks, but formation of such structural feature is more of an observation than the predictable design.

Although numerous noncentrosymmetric MOFs based on 1-D and related helical chains have been reported, it is far more difficult to predictably design SHG-active materials based on the 1-D systems owing to the lack of control along two other directions. Finally, noncentrosymmetric MOFs can be readily generated from either homochiral ligands or racemic mixtures of chiral liagnds. The chromophoric dipoles are not necessarily aligned in a noncentrosymmetric manner in these MOFs, and as a result, SHG responses from these MOFs have not been impressive.

The modular synthetic nature of MOFs has enabled the synthesis of numerous noncentrosymmetric, SHG-active materials since the first demonstration of the crystal engineering of noncenstrosymmetric diamondoid networks.[74] MOFs have undoubtedly emerged as a great platform for designing noncentrosymmetric solids with SHG properties. Some of the MOFs have already shown SHG efficiency much higher than that of the technologically important $LiNbO_3$. Future efforts must be devoted to careful evaluations of other key attributes of MOFs, such as chemical stability, mechanical strength, optical transparency, and phase matchability, in order to move these scientific discoveries into their potential technological applications in electro-optic devices.

AUTHOR INFORMATION

Corresponding Author

*Phone: 919-962-6320. Fax: 919-962-2388. E-mail: wlin@unc.edu.

Author Contributions

†These authors contributed equally.

BIOGRAPHIES

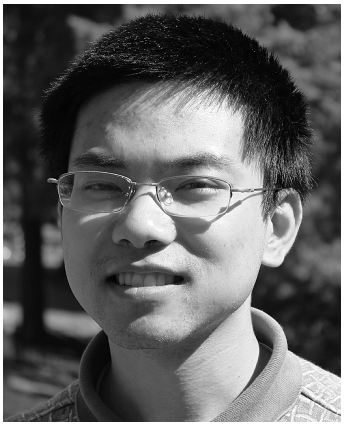

Cheng Wang obtained his B.S. degree from Peking University in 2009. He is currently a Ph.D. student at the University of North Carolina at Chapel Hill under the guidance of Professor Wenbin Lin. His research interests center on the development of framework materials for asymmetric catalysis and solar energy utilization.

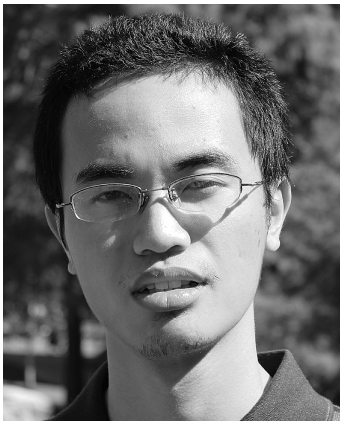

Teng Zhang obtained his B.S. degree from Peking University, China, in 2010 and is currently a graduate student at the University of North Carolina at Chapel Hill under the guidance of Professor Wenbin Lin. His research focuses on developing porous metal—organic frameworks for heterogeneous asymmetric catalysis.

Wenbin Lin is the Kenan Distinguished Professor of Chemistry and Pharmacy at the University of North Carolina at Chapel Hill. His research efforts focus on designing novel supramolecular systems and hybrid nanomaterials for applications in chemical and life sciences. He has published >180 papers in several research areas. (Group website: http://www.unc.edu/~wlin/.)

ACKNOWLEDGMENT

We thank the NSF for the support of this work. C.W. thanks the UNC Department of Chemistry for an Ernest L. Eliel fellowship.

LIST OF ABBREVIATIONS

AmTAZ	3-amino-1,2,4-triazol-4-ide
apa	(*E*)-3-amino-3-(pyridin-3-yl)acrylate
app	3-amino-3-(pyridin-3-yl)propanoate
aptz	5-(6-aminopyridin-3-yl)tetrazol-1-ide
3,3′-AZDB	3,3′-azodibenzoate
bbi	1,1′-(1,4-butanediyl)bis(imidazole)
BCDC	*N*,*N*′-bis(4-cyanophenyl)-(1*R*,2*R*)-diaminocyclohexane
bddp	(2*S*,2′*S*)-2,2′-(benzene-1,4-dicarboxamido)-dipropionate
bimb	4,4′-bis(imidazol-1-ylmethyl)biphenyl
bix	1,4-bis(imidazol-1-ylmethyl)benzene
bptc	3,3′,4,4′-biphenyltetracarboxylate
2,2′-bpy	2,2′-bipyridine
4,4′-bpy	4,4′-bipyridine
BTA	2-(1*H*-benzotriazol-1-yl)acetate
BTC	benzene-1,3,5-tricarboxylate
bte	1,2-bis(1,2,4-triazol-1-yl)ethane
bth	1,6-bis(1,2,4-triazol-1-yl)hexane
btp	1,3-bis(1,2,4-triazol-1-yl)propane
bza	benzoate
D-H_2ca	D-camphoric acid
cda	carbamyldicyanomethanide anion
ddm	*p*,*p*′-diaminodiphenylmethane
DMA	dimethylacetamide
DMF	*N*,*N*′-dimethylformamide
H_2dnty	3,5-dinitrotyrosine
DPA	2,2′-biphenyldicarboxylate
dpp	1,3-di(4-pyridyl)propane
eimnic	5-ethyl-2-(4-isopropyl-4-methyl-5-oxo-4,5-dihydro-imidazol-2-yl)nicotinate
datrz	3,5-diamino-1,2,4-triazol-1-ide
dicnq	6,7-dicyanodipyridoquinoxaline
dimb	3,5-di(imidazol-1-yl)benzoate
Etpvpp	ethyl (*E*)-(4-(2-(pyridin-3-yl)vinyl)phenyl)phosphonate
H_4FA	4,4′-(hexafluoroisopropylidene)diphthalic acid
$H_3$5-hiph	5-hydroxyisophthalic acid
$H_3$4-hiph	4-hydroxyisophthalic acid
H_2hnic	6-hydroxynicotinic acid
hpac	2-hydroxy-2-phosphonatoacetate
htb	hydrotris(1,2,4-triazolyl)borato
ima	2-(imidazol-1-yl)acetate
imac	(*E*)-3-(imidazol-4-yl)acrylate
imbi	2-(1-imidazolylmethyl)-1*H*-benzo[*d*]imidazole
inic	isonicotinate
iph	isophthalate
lac	*S*-(−)-lactate
mbix	1,3-bis(imidazol-1-ylmethyl)benzene
nic	nicotinate
obix	1,2-bis(imidazol-1-ylmethyl)benzene
odba	4,4′-oxidibenzoate
3,3′-ODPA	3,3′-oxidiphthalate
4,4′-ODPA	4,4′-oxidiphthalate
opyca	1-oxo-4-pyridylcarboxylate
pdbpt	5-(3-(2-(pyridin-4-yl)2,3-dihydro-1*H*-benzo[e]indol-1-yl)phenyl)tetrazol-1-ide
Hpdc	1*H*-pyrazole-3,5-dicarboxylate
2,3-PDCO	pyridine-2,3-dicarboxylate *N*-oxide
2,6-PDCO	pyridine-2,6-dicarboxylate *N*-oxide
pec	4-(2-(pyridin-4-yl)ethenyl)cinnamate
phen	1,10-phenanthroline
pht	phthalate
phtz	5-phenyltetrazol-2-ide
pic	picolinate
H_3PIDC	2-(pyridin-4-yl)-1*H*-imidazole-4,5-dicarboxylic acid
ppodz	2-(pyridin-2-yl)-5-(pyridin-4-yl)-1,3,4-oxadiazole
psmp	((phenylsulfonyl)methyl)phosphonate
ptmb	4-((pyridin-4-ylthio)methyl)benzoate
3-ptz	5-(pyridin-3-yl)tetrazol-2-ide
4-ptz	5-(pyridin-4-yl)tetrazol-2-ide
py	pyridine
3-pya	(*E*)-3-(pyridin-3-yl)acrylate

dx.doi.org/10.1021/cr200252n |*Chem. Rev.* 2012, 112, 1084–1104

4-pya	(*E*)-3-(pyridin-4-yl)acrylate
pyb	4-(pyridin-4-yl)benzoate
pydc	pyridine-3,4-dicarboxylate
pymt	pyrimidine-2-thiolate
(*E*)-2-pyv-3-bza	(*E*)-3-(2-(pyridin-2-yl)vinyl)benzoate
(*E*)-3-pyv-4-bza	(*E*)-4-(2-(pyridin-3-yl)vinyl)benzoate
(*Z*)-3-pyv-4-bza	(*Z*)-4-(2-(pyridin-3-yl)vinyl)benzoate
(*E*)-4-pyv-3-bza	(*E*)-3-(2-(pyridin-4-yl)vinyl)benzoate
(*E*)-4-pyv-4-bza	(*E*)-4-(2-(pyridin-4-yl)vinyl)benzoate
(*E*)-3-pyv-5-tpa	(*E*)-5-[2-(3-pyridyl)vinyl]thiophene-2-carboxylate
pyz	pyrazine
quin-6-c	quinoline-6-carboxylate
H_2SCMC	*S*-carboxymethyl-L-cysteine
SDBA	4,4′-sulfonyldibenzoate
SDP	4,4′-sulfonyldiphthalate
SIP	5-sulfonatoisophthalate
SPA	4-sulfo-L-phenylalanine
suc	succinate
H_4tart	tartaric acid
tcom	tetrakis(4-(carboxyphenyl)oxamethyl)methane
tcsm	tetrakis(4-(carboxylatostyrenyl))methane
tdea	tri(2-(2,3-dimethoxybenzamido)ethyl)amine
timb	1,3,5-tris(imidazol-1-ylmethyl)-2,4,6-trimethylbenzene
tpb	tris(2,3,5,6-tetramethyl-4-(pyridin-4-yl)phenyl)borane
tpcc	(1*R*,3*S*)-1,2,2-trimethyl-3-(pyridin-4-ylcarbamoyl)cyclopentanecarboxylate
Htrtr	3-(1,2,4-triazol-4-yl)-1*H*-1,2,4-triazole
H_2tzb	4-(1*H*-tetrazol-5-yl)butanoic acid
tzpbin	1-(3-(1*H*-tetrazol-5-yl)phenyl)-2-(pyridin-4-yl)-3*H*-benzo[e]indole

REFERENCES

(1) Nikogosian, D. N. In *Nonlinear optical crystals: a complete survey*; Springer-Science: New York, 2005.
(2) Jain, K.; Pratt, G. W. *Appl. Phys. Lett.* **1976**, *28*, 719.
(3) Franken, P. A.; Hill, A. E.; Peters, C. W.; Weinreich, G. *Phys. Rev. Lett.* **1961**, *7*, 118.
(4) Boyd, R. W. *Nonlinear Optics*, 3rd ed.; Academic Press: Burlington, 2008.
(5) Nye, J. F. *Physical properties of crystals: their representation by tensors and matrices*; Clarendon: Oxford, 1985.
(6) Kleinman, D. A. *Phys. Rev.* **1962**, *126*, 1977.
(7) Prasad, P. N.; Williams, D. J. *Introduction to nonlinear optical effects in molecules and polymers*; John Wiley & Sons, Inc.: New York, 1991.
(8) Pan, S.; Smit, J. P.; Watkins, B.; Marvel, M. R.; Stern, C. L.; Poeppelmeier, K. R. *J. Am. Chem. Soc.* **2006**, *128*, 11631.
(9) Wu, H.; Pan, S.; Poeppelmeier, K. R.; Li, H.; Jia, D.; Chen, Z.; Fan, X.; Yang, Y.; Rondinelli, J. M.; Luo, H. *J. Am. Chem. Soc.* **2011**, *133*, 7786.
(10) Becker, P. *Adv. Mater.* **1998**, *10*, 979.
(11) Keszler, D. A. *Curr. Opin. Solid State Mater. Sci.* **1999**, *4*, 155.
(12) Nicholls, J. F. H.; Henderson, B.; Chai, B. H. T. *Opt. Mater.* **2001**, *16*, 453.
(13) Halasyamani, P. S. *Chem. Mater.* **2004**, *16*, 3586.
(14) Ok, K. M.; Halasyamani, P. S.; Casanova, D.; Llunell, M.; Alemany, P.; Alvarez, S. *Chem. Mater.* **2006**, *18*, 3176.
(15) Halasyamani, P. S.; Poeppelmeier, K. R. *Chem. Mater.* **1998**, *10*, 2753.
(16) Sun, C. F.; Hu, C. L.; Xu, X.; Ling, J. B.; Hu, T.; Kong, F.; Long, X. F.; Mao, J. G. *J. Am. Chem. Soc.* **2009**, *131*, 9486.
(17) Radhakrishnan, T. P. *Acc. Chem. Res.* **2008**, *41*, 367.
(18) Le Bozec, H.; Renouard, T. *Eur. J. Inorg. Chem.* **2000**, *2000*, 229.
(19) Liao, Y.; Eichinger, B. E.; Firestone, K. A.; Haller, M.; Luo, J.; Kaminsky, W.; Benedict, J. B.; Reid, P. J.; Jen, A. K. Y.; Dalton, L. R.; Robinson, B. H. *J. Am. Chem. Soc.* **2005**, *127*, 2758.
(20) Di Bella, S. *Chem. Soc. Rev.* **2001**, *30*, 355.
(21) Wampler, R. D.; Begue, N. J.; Simpson, G. J. *Cryst. Growth Des.* **2008**, *8*, 2589.
(22) Evans, O. R.; Lin, W. *Acc. Chem. Res.* **2002**, *35*, 511.
(23) Cox, S. D.; Gier, T. E.; Stucky, G. D.; Bierlein, J. *J. Am. Chem. Soc.* **1988**, *110*, 2986.
(24) Cox, S.; Gier, T.; Stucky, G. *Chem. Mater.* **1990**, *2*, 609.
(25) Werner, L.; Caro, J.; Finger, G.; Kornatowski, J. *Zeolites*, *12*, 658.
(26) Reck, G.; Marlow, F.; Kornatowski, J.; Hill, W.; Caro, J. *J. Phys. Chem.* **1996**, *100*, 1698.
(27) Kim, H. S.; Lee, S. M.; Ha, K.; Jung, C.; Lee, Y.-J.; Chun, Y. S.; Kim, D.; Rhee, B. K.; Yoon, K. B. *J. Am. Chem. Soc.* **2003**, *126*, 673.
(28) Kim, H. S.; Sohn, K. W.; Jeon, Y.; Min, H.; Kim, D.; Yoon, K. B. *Adv. Mater.* **2007**, *19*, 260.
(29) Meredith, G. R.; VanDusen, J.; Williams, D. J. *Macromolecules* **1982**, *15*, 1385.
(30) Burland, D. M.; Miller, R. D.; Walsh, C. A. *Chem. Rev.* **1994**, *94*, 31.
(31) Dalton, L. R.; Harper, A. W.; Ghosn, R.; Steier, W. H.; Ziari, M.; Fetterman, H.; Shi, Y.; Mustacich, R. V.; Jen, A. K. Y.; Shea, K. J. *Chem. Mater.* **1995**, *7*, 1060.
(32) Luo, J.; Haller, M.; Li, H.; Kim, T. D.; Jen, A. K. Y. *Adv. Mater.* **2003**, *15*, 1635.
(33) Yesodha, S. K.; Sadashiva Pillai, C. K.; Tsutsumi, N. *Prog. Polym. Sci.* **2004**, *29*, 45.
(34) Saadeh, H.; Yu, D.; M. Wang, L.; P. Yu, L. *J. Mater. Chem.* **1999**, *9*, 1865.
(35) Luo, J.; Liu, S.; Haller, M.; Liu, L.; Ma, H.; Jen, A. K. Y. *Adv. Mater.* **2002**, *14*, 1763.
(36) Shan, B. Z.; Bai, Z. P.; Chen, Y.; You, X. Z.; Cai, Z. G.; Yang, P. Q. *Supramol. Sci.* **1998**, *5*, 499.
(37) Popovitz-Biro, R.; Hill, K.; Landau, E. M.; Lahav, M.; Leiserowitz, L.; Sagiv, J.; Hsiung, H.; Meredith, G. R.; Vanherzeele, H. *J. Am. Chem. Soc.* **1988**, *110*, 2672.
(38) Ashwell, G. J.; Hargreaves, R. C.; Baldwin, C. E.; Bahra, G. S.; Brown, C. R. *Nature* **1992**, *357*, 393.
(39) Penner, T. L.; Motschmann, H. R.; Armstrong, N. J.; Ezenyilimba, M. C.; Williams, D. J. *Nature* **1994**, *367*, 49.
(40) Li, D.; Ratner, M. A.; Marks, T. J.; Zhang, C.; Yang, J.; Wong, G. K. *J. Am. Chem. Soc.* **1990**, *112*, 7389.
(41) Lin, W.; Lin, W.; Wong, G. K.; Marks, T. J. *J. Am. Chem. Soc.* **1996**, *118*, 8034.
(42) Lin, W.; Yitzchaik, S.; Lin, W. P.; Malik, A.; Durbin, M. K.; Richter, A. G.; Wong, G. K.; Dutta, P.; Marks, T. J. *Angew. Chem., Int. Ed.* **1995**, *34*, 1497.
(43) Lin, W.; Lee, T.-L.; Lyman, P. F.; Lee, J.; Bedzyk, M. J.; Marks, T. J. *J. Am. Chem. Soc.* **1997**, *119*, 2205.
(44) Malik, A.; Lin, W.; Durbin, M. K.; Marks, T. J.; Dutta, P. *J. Chem. Phys.* **1997**, *107*, 645.
(45) Katz, H. E.; Wilson, W. L.; Scheller, G. *J. Am. Chem. Soc.* **1994**, *116*, 6636.
(46) Katz, H. E.; Scheller, G.; Putvinski, T. M.; Schilling, M. L.; Wilson, W. L.; Chidsey, C. E. *Science* **1991**, *254*, 1485.
(47) Duarte, F. J. In *Tunable Laser Applications*, 2nd ed.; Duarte, F. J., Ed.; CRC: New York, 2009.
(48) Rice, A.; Jin, Y.; Ma, X. F.; Zhang, X. C.; Bliss, D.; Larkin, J.; Alexander, M. *Appl. Phys. Lett.* **1994**, *64*, 1324.
(49) Han, M.; Giese, G.; Bille, J. F. *Opt. Express* **2005**, *13*, 5791.
(50) Brown, D. J.; Morishige, N.; Neekhra, A.; Minckler, D. S.; Jester, J. V. *J. Biomed. Opt.* **2007**, 12.
(51) Byer, R. L.; Harris, S. E. *Phys. Rev.* **1968**, *168*, 1064.
(52) Faust, W. L.; Henry, C. H. *Phys. Rev. Lett.* **1966**, *17*, 1265.

(53) Maker, P. D.; Terhune, R. W.; Nisenoff, M.; Savage, C. M. *Phys. Rev. Lett.* **1962**, *8*, 21.
(54) Kurtz, S. K. In *Quantum Electronics: A Treatise*; Rabin, H., Tang, C. L., Eds.; Academic Press, Inc.: New York, 1975; Vol. 1, p 209.
(55) Kurtz, S. K.; Perry, T. T. *J. Appl. Phys.* **1968**, *39*, 3798.
(56) Ok, K. M.; Chi, E. O.; Halasyamani, P. S. *Chem. Soc. Rev.* **2006**, *35*, 710.
(57) Coe, B. J. In *Comprehensive Coordination Chemistry II: From Biology to Nanotechnology*; McCleverty, J. A., Meyer, T. J., Eds.; Pergamon: Oxford, 2003; Vol. 9, p 624.
(58) Ferey, G.; Mellot-Draznieks, C.; Serre, C.; Millange, F. *Acc. Chem. Res.* **2005**, *38*, 217.
(59) Kitagawa, S.; Kitaura, R.; Noro, S. *Angew. Chem., Int. Ed.* **2004**, *43*, 2334.
(60) Rowsell, J. L.; Yaghi, O. M. *Angew. Chem., Int. Ed.* **2005**, *44*, 4670.
(61) Xie, Z.; Ma, L.; deKrafft, K. E.; Jin, A.; Lin, W. *J. Am. Chem. Soc.*, *132*, 922.
(62) Chen, B.; Wang, L.; Xiao, Y.; Fronczek, F. R.; Xue, M.; Cui, Y.; Qian, G. *Angew. Chem., Int. Ed.* **2009**, *48*, 500.
(63) Lan, A.; Li, K.; Wu, H.; Olson, D. H.; Emge, T. J.; Ki, W.; Hong, M.; Li, J. *Angew. Chem., Int. Ed.* **2009**, *48*, 2334.
(64) Lee, J.; Farha, O. K.; Roberts, J.; Scheidt, K. A.; Nguyen, S. T.; Hupp, J. T. *Chem. Soc. Rev.* **2009**, *38*, 1450.
(65) Wu, C. D.; Hu, A.; Zhang, L.; Lin, W. *J. Am. Chem. Soc.* **2005**, *127*, 8940.
(66) Liu, D.; Huxford, R. C.; Lin, W. *Angew. Chem., Int. Ed.* **2011**, *50*, 3696.
(67) Lin, W.; Rieter, W. J.; Taylor, K. M. *Angew. Chem., Int. Ed.* **2009**, *48*, 650.
(68) Della Rocca, J.; Lin, W. *Eur. J. Inorg. Chem.* **2010**, 3725.
(69) Rieter, W. J.; Pott, K. M.; Taylor, K. M.; Lin, W. *J. Am. Chem. Soc.* **2008**, *130*, 11584.
(70) Huxford, R. C.; Della Rocca, J.; Lin, W. B. *Curr. Opin. Chem. Biol.* **2010**, *14*, 262.
(71) Ma, S. Q.; Fillinger, J. A.; Ambrogio, M. W.; Zuo, J. L.; Zhou, H. C. *Inorg. Chem. Commun.* **2007**, *10*, 220.
(72) Lin, Z.; Jiang, F.; Chen, L.; Yuan, D.; Hong, M. *Inorg. Chem.* **2004**, *44*, 73.
(73) Du, Z. Y.; Sun, Y. H.; Xu, X. A.; Xu, G. H.; Xie, Y. R. *Eur. J. Inorg. Chem.* **2010**, 4865.
(74) Evans, O. R.; Xiong, R. G.; Wang, Z. Y.; Wong, G. K.; Lin, W. *Angew. Chem., Int. Ed.* **1999**, *38*, 536.
(75) Evans, O. R.; Wang, Z.; Xiong, R.-G.; Foxman, B. M.; Lin, W. *Inorg. Chem.* **1999**, *38*, 2969.
(76) Lin, W.; Ma, L.; Evans, O. R. *Chem. Commun.* **2000**, 2263.
(77) Evans, O. R.; Lin, W. *Chem. Mater.* **2001**, *13*, 2705.
(78) Feng, X.; Wen, Y. H.; Lan, Y. Z.; Feng, Y. L.; Pan, C. Y.; Yao, Y. G. *Inorg. Chem. Commun.* **2009**, *12*, 89.
(79) Lin, J. D.; Long, X. F.; Lin, P.; Du, S. W. *Cryst. Growth Des.* **2010**, *10*, 146.
(80) Wang, Y. T.; Tang, G. M.; Wu, Y.; Qin, X. Y.; Qin, D. W. *J. Mol. Struct.* **2007**, *831*, 61.
(81) Zhao, H.; Qu, Z.-R.; Ye, H.-Y.; Xiong, R.-G. *Chem. Soc. Rev.* **2008**, *37*, 84.
(82) Wu, M. F.; Xu, G.; Zheng, F. K.; Liu, Z. F.; Wang, S. H.; Guo, G. C.; Huang, J. S. *Inorg. Chem. Commun.* **2011**, *14*, 333.
(83) Ye, Q.; Li, Y. H.; Song, Y. M.; Huang, X. F.; Xiong, R. G.; Xue, Z. L. *Inorg. Chem.* **2005**, *44*, 3618.
(84) Wang, L.-Z.; Qu, Z.-R.; Zhao, H.; Wang, X.-S.; Xiong, R.-G.; Xue, Z.-L. *Inorg. Chem.* **2003**, *42*, 3969.
(85) Liang, L. L.; Ren, S. B.; Zhang, J.; Li, Y. Z.; Du, H. B.; You, X. Z. *Dalton Trans.* **2010**, *39*, 7723.
(86) Guo, Z. G.; Cao, R.; Wang, X.; Li, H. F.; Yuan, W. B.; Wang, G. J.; Wu, H. H.; Li, J. *J. Am. Chem. Soc.* **2009**, *131*, 6894.
(87) Qu, Z.-R.; Zhao, H.; Wang, Y.-P.; Wang, X.-S.; Ye, Q.; Li, Y.-H.; Xiong, R.-G.; Abrahams, B. F.; Liu, Z.-G.; Xue, Z.-L.; You, X.-Z. *Chem.—Eur. J.* **2004**, *10*, 53.
(88) Chen, Z.-F.; Xiong, R.-G.; Abrahams, B. F.; You, X.-Z.; Che, C.-M. *J. Chem. Soc., Dalton Trans.* **2001**, 2453.
(89) Ayyappan, P.; Evans, O. R.; Cui, Y.; Wheeler, K. A.; Lin, W. *Inorg. Chem.* **2002**, *41*, 4978.
(90) Zhou, Y. F.; Yuan, D. Q.; Wu, B. L.; Wang, R. H.; Hong, M. C. *New J. Chem.* **2004**, *28*, 1590.
(91) Kang, Y.; Yao, Y.-G.; Qin, Y.-Y.; Zhang, J.; Chen, Y.-B.; Li, Z.-J.; Wen, Y.-H.; Cheng, J.-K.; Hu, R.-F. *Chem. Commun.* **2004**, 1046.
(92) Zhang, L.; Qin, Y. Y.; Li, Z. J.; Lin, Q. P.; Cheng, J. K.; Zhang, J.; Yao, Y. G. *Inorg. Chem.* **2008**, *47*, 8286.
(93) Wang, Y.-T.; Fan, H.-H.; Wang, H.-Z.; Chen, X.-M. *Inorg. Chem.* **2005**, *44*, 4148.
(94) Pan, J. G.; Zhang, G. J.; Zheng, Y. Q.; Lin, J. L.; Xu, W. *J. Cryst. Growth* **2007**, *308*, 89.
(95) Chu, Q.; Liu, G. X.; Huang, Y. Q.; Wang, X. F.; Sun, W. Y. *Dalton Trans.* **2007**, 4302.
(96) Su, Z.; Bai, Z. S.; Xu, J.; Okamura, T. A.; Liu, G. X.; Chu, Q.; Wang, X. F.; Sun, W. Y.; Ueyama, N. *CrystEngComm* **2009**, *11*, 873.
(97) Liu, C. M.; Zuo, J. L.; Zhang, D. Q.; Zhu, D. B. *CrystEngComm* **2008**, *10*, 1674.
(98) Liu, G. X.; Zhu, K.; Chen, H.; Huang, R. Y.; Ren, X. M. *Z. Anorg. Allg. Chem.* **2009**, *635*, 156.
(99) Liu, G. X.; Huang, R. Y.; Huang, L. F.; Kong, X. J.; Ren, X. M. *CrystEngComm* **2009**, *11*, 643.
(100) Wang, Y. T.; Tang, G. M.; Wei, Y. Q.; Qin, T. X.; Li, T. D.; He, C.; Ling, J. B.; Long, X. F.; Ng, S. W. *Cryst. Growth Des.* **2010**, *10*, 25.
(101) Liu, G. X.; Zhu, K.; Xu, H. M.; Nishihara, S.; Huang, R. Y.; Ren, X. M. *CrystEngComm* **2010**, *12*, 1175.
(102) Chen, L. Z.; Huang, Y.; Xiong, R. G.; Hu, H. W. *J. Mol. Struct.* **2010**, *963*, 16.
(103) Liu, Q.-Y.; Wang, Y.-L.; Shan, Z.-M.; Cao, R.; Jiang, Y.-L.; Wang, Z.-J.; Yang, E.-L. *Inorg. Chem.* **2010**, *49*, 8191.
(104) Zheng, Y. Q.; Zhang, J.; Liu, J. Y. *CrystEngComm* **2010**, *12*, 2740.
(105) Wang, F.; Zhang, J.; Yu, R. M.; Chen, S. M.; Wu, X. Y.; Chen, S. C.; Xie, Y. M.; Zhou, W. W.; Lu, C. Z. *CrystEngComm* **2010**, *12*, 671.
(106) Lin, J. D.; Wu, S. T.; Li, Z. H.; Du, S. W. *Dalton Trans.* **2010**, *39*, 10719.
(107) Wong, K.-L.; Law, G.-L.; Kwok, W.-M.; Wong, W.-T.; Phillips, D. L. *Angew. Chem., Int. Ed.* **2005**, *44*, 3436.
(108) Di Bella, S.; Fragala, I.; Ledoux, I.; Zyss, J. *Chem.—Eur. J.* **2001**, *7*, 3738.
(109) Lin, W.; Wang, Z. Y.; Ma, L. *J. Am. Chem. Soc.* **1999**, *121*, 11249.
(110) Liu, Y.; Li, G.; Li, X.; Cui, Y. *Angew. Chem., Int. Ed.* **2007**, *46*, 6301.
(111) Liu, Y.; Xu, X.; Zheng, F. K.; Cui, Y. *Angew. Chem., Int. Ed.* **2008**, *47*, 4538.
(112) Lin, W.; Evans, O. R.; Xiong, R. G.; Wang, Z. Y. *J. Am. Chem. Soc.* **1998**, *120*, 13272.
(113) Evans, O. R.; Lin, W. *Chem. Mater.* **2001**, *13*, 3009.
(114) Xie, Y.-R.; Zhao, H.; Wang, X.-S.; Qu, Z.-R.; Xiong, R.-G.; Xue, X.; Xue, Z.; You, X.-Z. *Eur. J. Inorg. Chem.* **2003**, *2003*, 3712.
(115) Shi, J.-m.; Xu, W.; Liu, Q.-y.; Liu, F.-l.; Huang, Z.-l.; Lei, H.; Yu, W.-t.; Fang, Q. *Chem. Commun.* **2002**, 756.
(116) He, Y. H.; Lan, Y. Z.; Zhan, C. H.; Feng, Y. L.; Su, H. *Inorg. Chim. Acta* **2009**, *362*, 1952.
(117) Zhang, X.-M.; Chen, J.-S.; Xu, K.-Y.; Ding, C.-R.; She, W.-L.; Chen, X.-M. *Inorg. Chim. Acta* **2004**, *357*, 1389.
(118) Wen, L. L.; Dang, D. B.; Duan, C. Y.; Li, Y. Z.; Tian, Z. F.; Meng, Q. J. *Inorg. Chem.* **2005**, *44*, 7161.
(119) Janiak, C.; Scharmann, T. G.; Albrecht, P.; Marlow, F.; Macdonald, R. *J. Am. Chem. Soc.* **1996**, *118*, 6307.
(120) Ayyappan, P.; Sirokman, G.; Evans, O. R.; Warren, T. H.; Lin, W. *Inorg. Chim. Acta* **2004**, *357*, 3999.
(121) Hang, T.; Fu, D. W.; Ye, Q.; Xiong, R. G. *Cryst. Growth Des.* **2009**, *9*, 2026.
(122) Chen, Y. B.; Zhang, J.; Cheng, J. K.; Kang, Y.; Li, Z. J.; Yao, Y. G. *Inorg. Chem. Commun.* **2004**, *7*, 1139.

(123) Wang, Y.-T.; Tong, M.-L.; Fan, H.-H.; Wang, H.-Z.; Chen, X.-M. *Dalton Trans.* **2005**, 424.
(124) Wang, Y. T.; Tang, G. M.; Wei, Y. Q.; Qin, T. X.; Li, T. D.; Ling, J. B.; Long, X. F. *Inorg. Chem. Commun.* **2009**, *12*, 1164.
(125) Chen, H. F.; Guo, G. C.; Wang, M. S.; Xu, G.; Zou, W. Q.; Guo, S. P.; Wu, M. F.; Huang, J. S. *Dalton Trans.* **2009**, 10166.
(126) Zhang, J.; Li, Z. J.; Cao, X. Y.; Yao, Y. G. *J. Mol. Struct.* **2005**, *750*, 39.
(127) Han, L.; Hong, M.; Wang, R.; Wu, B.; Xu, Y.; Lou, B.; Lin, Z. *Chem. Commun.* **2004**, 2578.
(128) Liu, G. X.; Zhu, K.; Xu, H. M.; Nishihara, S.; Huang, R. Y.; Ren, X. M. *CrystEngComm* **2009**, *11*, 2784.
(129) Zhang, H.; Wang, X.; Teo, B. K. *J. Am. Chem. Soc.* **1996**, *118*, 11813.
(130) Zhang, H.; Wang, X.; Zhang, K.; Teo, B. K. *Coord. Chem. Rev.* **1999**, *183*, 157.
(131) Maggard, P. A.; Stern, C. L.; Poeppelmeier, K. R. *J. Am. Chem. Soc.* **2001**, *123*, 7742.
(132) Zang, S. Q.; Su, Y.; Li, Y. Z.; Ni, Z. P.; Meng, Q. J. *Inorg. Chem.* **2006**, *45*, 174.
(133) Wen, L. L.; Lu, Z. D.; Ren, X. M.; Duan, C. Y.; Meng, Q. J.; Gao, S. *Cryst. Growth Des.* **2009**, *9*, 227.
(134) Han, L.; Hong, M.; Wang, R.; Luo, J.; Lin, Z.; Yuan, D. *Chem. Commun.* **2003**, 2580.
(135) Xiong, R.-G.; Xue, X.; Zhao, H.; You, X.-Z.; Abrahams, B. F.; Xue, Z. *Angew. Chem., Int. Ed.* **2002**, *41*, 3800.
(136) Evans, O. R.; Wang, Z. Y.; Lin, W. *Chem. Commun.* **1999**, 1903.
(137) Li, W.; Jia, H. P.; Ju, Z. F.; Zhang, J. *Cryst. Growth Des.* **2006**, *6*, 2136.
(138) Hu, S.; Zou, H. H.; Zeng, M. H.; Wang, Q. X.; Liang, H. *Cryst. Growth Des.* **2008**, *8*, 2346.
(139) Zhou, W. W.; Chen, J. T.; Xu, G.; Wang, M. S.; Zou, J. P.; Long, X. F.; Wang, G. J.; Guo, G. C.; Huang, J. S. *Chem. Commun.* **2008**, 2762.
(140) Liu, T. F.; Lu, J.; Guo, Z. G.; Proserpio, D. M.; Cao, R. *Cryst. Growth Des.* **2010**, *10*, 1489.
(141) Zhang, R. B.; Li, Z. J.; Qin, Y. Y.; Cheng, J. K.; Zhang, J.; Yao, Y. G. *Inorg. Chem.* **2008**, *47*, 4861.
(142) Zhou, X. H.; Du, X. D.; Li, G. N.; Zuo, J. L.; You, X. Z. *Cryst. Growth Des.* **2009**, *9*, 4487.
(143) Liu, L.; Huang, S. P.; Yang, G. D.; Zhang, H.; Wang, X. L.; Fu, Z. Y.; Dai, J. C. *Cryst. Growth Des.* **2010**, *10*, 930.
(144) Anthony, S. P.; Radhakrishnan, T. P. *Cryst. Growth Des.* **2004**, *4*, 1223.
(145) Anthony, S. P.; Radhakrishnan, T. P. *Chem. Commun.* **2004**, 1058.
(146) Zhang, H. T.; Li, Y. Z.; Wang, T. W.; Nfor, E. N.; Wang, H. Q.; You, X. Z. *Eur. J. Inorg. Chem.* **2006**, 3532.
(147) Saha, R.; Biswas, S.; Mostafa, G. *CrystEngComm* **2011**, *13*, 1018.
(148) Liang, X. Q.; Li, D. P.; Zhou, X. H.; Sui, Y.; Li, Y. Z.; Zuo, J. L.; You, X. Z. *Cryst. Growth Des.* **2009**, *9*, 4872.
(149) Huang, Q. A.; Yu, J. C.; Gao, J. K.; Rao, X. T.; Yang, X. L.; Cui, Y. J.; Wu, C. D.; Zhang, Z. J.; Xiang, S. C.; Chen, B. L.; Qian, G. D. *Cryst. Growth Des.* **2010**, *10*, 5291.
(150) Xu, W.; Liu, W.; Yao, F. Y.; Zheng, Y. Q. *Inorg. Chim. Acta* **2011**, *365*, 297.
(151) Wang, Y.-T.; Fan, H.-H.; Wang, H.-Z.; Chen, X.-M. *J. Mol. Struct.* **2005**, *740*, 61.
(152) Xiong, R. G.; Zuo, J. L.; You, X. Z.; Fun, H. K.; Raj, S. S. S. *New J. Chem.* **1999**, *23*, 1051.
(153) Xie, Y. R.; Xiong, R. G.; Xue, X.; Chen, X. T.; Xue, Z. L.; You, X. Z. *Inorg. Chem.* **2002**, *41*, 3323.
(154) Ye, Q.; Li, Y.-H.; Wu, Q.; Song, Y.-M.; Wang, J.-X.; Zhao, H.; Xiong, R.-G.; Xue, Z. *Chem.—Eur. J.* **2005**, *11*, 988.
(155) Fu, R. B.; Zhang, H. S.; Wang, L. S.; Hu, S. M.; Li, Y. M.; Huang, X. H.; Wu, X. T. *Eur. J. Inorg. Chem.* **2005**, 3211.
(156) Fu, D.-W.; Zhang, W.; Xiong, R.-G. *Dalton Trans.* **2008**, 3946.
(157) Ye, Q.; Tang, Y.-Z.; Wang, X.-S.; Xiong, R.-G. *Dalton Trans.* **2005**, 1570.